THE JOURNAL OF BIOLOGICAL CHEMISTRY VOL. 292, NO. 15, pp. 6352–6368, April 14, 2017

Heterodimers of serotonin receptor subtypes 2 are driven by 5-HT_{2C} protomers

Received for publication, January 30, 2017, and in revised form, March 2, 2017 Published, JBC Papers in Press, March 3, 2017, DOI 10.1074/jbc.M117.779041

Imane Moutkine[‡§¶1], Emily Quentin[‡§¶1], Bruno P. Guiard[‖], Luc Maroteaux[‡§¶2], and Stephane Doly[‡‡§§3]**

From the [‡]INSERM UMR-S839, Paris 75005, the [§]Université Pierre et Marie Curie, Paris 75005, the [¶]Institut du Fer à Moulin, Paris 75005, the [**]Institut Cochin, INSERM U1016, CNRS UMR8104, Paris 75014, the [‡‡]Université Paris Descartes, Sorbonne Paris Cité, Paris 75014, the [§§]Université Clermont Auvergne, INSERM, NEURO-DOL, F-63000 Clermont-Ferrand, and the [‖]Research Center on Animal Cognition, Center for Integrative Biology, Université Paul Sabatier, UMR5169 CNRS, 118, Route de Narbonne, 31062, Toulouse Cedex 9, France

Edited by Henrik G. Dohlman

The serotonin receptor subtypes 2 comprise 5-HT_{2A}, 5-HT_{2B}, and 5-HT_{2C}, which are Gα_q-coupled receptors and display distinct pharmacological properties. Although co-expressed in some brain regions and involved in various neurological disorders, their functional interactions have not yet been studied. We report that 5-HT_2 receptors can form homo- and heterodimers when expressed alone or co-expressed in transfected cells. Co-immunoprecipitation and bioluminescence resonance energy transfer studies confirmed that 5-HT_{2C} receptors interact with either 5-HT_{2A} or 5-HT_{2B} receptors. Although heterodimerization with 5-HT_{2C} receptors does not alter 5-HT_{2C} Gα_q-dependent inositol phosphate signaling, 5-HT_{2A} or 5-HT_{2B} receptor-mediated signaling was totally blunted. This feature can be explained by a dominance of 5-HT_{2C} on 5-HT_{2A} and 5-HT_{2B} receptor binding; in 5-HT_{2C}-containing heterodimers, ligands bind and activate the 5-HT_{2C} protomer exclusively. This dominant effect on the associated protomer was also observed in neurons, supporting the physiological relevance of 5-HT_2 receptor heterodimerization *in vivo*. Accordingly, exogenous expression of an inactive form of the 5-HT_{2C} receptor in the locus ceruleus is associated with decreased 5-HT_{2A}-dependent noradrenergic transmission. These data demonstrate that 5-HT_2 receptors can form functionally asymmetric heterodimers *in vitro* and *in vivo* that must be considered when analyzing the physiological or pathophysiological roles of serotonin in tissues where 5-HT_2 receptors are co-expressed.

Many members of the G-protein-coupled receptor (GPCR)[4] family have the capacity to form homo- or hetero-oligomers with biochemical and functional characteristics, including receptor pharmacology, signaling, and regulation, which are unique to these oligomeric conformations. These GPCR oligomers have been found not only to occur within a type of GPCR but also across different families and subtypes (1, 2).

Metabotropic serotonin (5-hydroxytryptamine, 5-HT) subtype 2 receptors (5-HT_2), which belong to the class A-1 GPCR family, display a widespread expression in the nervous system and are involved in an important array of physiological and pathological processes. The 5-HT_2 subfamily consists of three Gα_q/Gα_{11}-coupled receptors, 5-HT_{2A}, 5-HT_{2B}, and 5-HT_{2C}, which mediate excitatory neurotransmission (3). Interestingly, 5-HT_2 subtypes coexist in multiple areas of the brain (4, 5). For example, 5-HT_{2A} and 5-HT_{2C} receptors are co-expressed in GABAergic interneurons and in a subpopulation of pyramidal neurons of the PFC (6–8), in dopaminergic neurons of the ventral tegmental area (9, 10), and 5-HT_{2C} and 5-HT_{2B} receptors are expressed in pro-opiomelanocortin (POMC) neurons of the hypothalamic arcuate nucleus (11). Although 5-HT_2 receptors are similar in structure, there are differences in their pharmacology and signaling outputs (12). It has been reported that 5-HT_{2A} and 5-HT_{2C} receptors can function as stable homodimers (13–16), whereas the existence of 5-HT_{2B} homodimers has not yet been documented. Dimers have also been reported

This work was supported by funds from the Centre National de la Recherche Scientifique, Institut National de la Santé et de la Recherche Médicale, the Université Pierre et Marie Curie, the Université Paris Descartes, grants from the Fondation de France, Fondation pour la Recherche Médicale "Equipe FRM DEQ2014039529," and the French Ministry of Research (Agence Nationale pour la Recherche Grant ANR-12-BSV1-0015-01 and the Investissements d'Avenir Programme Grant ANR-11-IDEX-0004-02). The L. M. team is part of the École des Neurosciences de Paris Ile-de-France network and the Bio-Psy Labex, and as such this work was supported by French state funds managed by the ANR within the Investissements d'Avenir programme under Reference ANR-11-IDEX-0004-02. The authors declare that they have no conflicts of interest with the contents of this article.

[1] Both authors contributed equally to this work.
[2] To whom correspondence may be addressed. E-mail: Luc.maroteaux@upmc.fr.
[3] To whom correspondence may be addressed: Université Clermont Auvergne, INSERM, NEURO-DOL, F-63000 Clermont-Ferrand, France. E-mail: stephane.doly@inserm.fr.

[4] The abbreviations used are: GPCR, G-protein-coupled receptor; LC, locus coeruleus; 5-HT, serotonin, 5-hydroxytryptamine; DOI, (±)-2,5-dimethoxy-4-iodoamphetamine hydrochloride; NDF, nor-(+)-fenfluramine; IP, inositol phosphate; ΔCter, C-terminal deletion; Rluc, *Renilla* luciferase; DSP4, *N*-(2-chloroethyl)-*N*-ethyl-2-bromobenzylamine; RS127445, 2-amino-4-(4-fluoronaphth-1-yl)-6-isopropylpyrimidine hydrochloride; RS102221, 8-[5-(2,4-dimethoxy-5-(4-trifluoromethylphenylsulfonamido)phenyl-5-oxopentyl)]-1,3,8-triazaspiro[4.5]de cane-2,4-dione hydrochloride; SB242084, [6-chloro-5-methyl-1-(6-(2-methylpiridin-3-yloxy)pyridine-3-yl carbamoyl] inodoline dihydrochloride); MDL100907, *R*-(+)-α-(2,3-dimethoxyphenyl)-1-[2-(4-fluorophenylethyl)]-4-piperidine methanol; AAV, adeno-associated virus; IRES, internal ribosome entry site; DR, dorsal raphe; PLC, phospholipase C; BisTris, 2-[bis(2-hydroxyethyl)amino]-2-(hydroxymethyl)propane-1,3-diol; ANOVA, analysis of variance; PFC, prefrontal cortex; POMC, pro-opiomelanocortin; BRET, bioluminescence resonance energy transfer; IP_1, inositol 1-phosphate; IP_2, inositol 4,5-bisphosphate; IP_3, inositol 1,4,5-trisphosphate; LAD, lysergic acid diethylamide; HTRF, homogeneous time-resolved fluorescence; RA, activity ratio.

for other 5-HT receptors, including 5-HT$_{1A}$, 5-HT$_{1B}$, 5-HT$_{1D}$, 5-HT$_4$, and 5-HT$_7$ receptor subtypes in heterologous expression systems (13, 17–20). In addition, there are observations suggesting that the 5-HT$_2$ receptor subfamily can form heterodimeric complexes with other types of GPCRs. For example, the formation of heterodimers has been reported for the 5-HT$_{2A}$ with mGluR2, D$_2$-dopamine, and CB1 receptors (21–23), for 5-HT$_{2C}$ with ghrelin receptors (GHS-R1a) (24) and MT2 receptor (25), for 5-HT$_{1A}$ with μ-opioid (26) and adenosine A$_{2A}$ receptors (27), and for 5-HT$_{2B}$ with angiotensin AT1 receptors (28).

As mentioned above, oligomerization can occur between receptors of different GPCR families (*i.e.* 5-HT and dopamine for example) but also within the same family. A seminal study reported the identification of the first heterodimer between the 5-HT$_{1B}$ and 5-HT$_{1D}$ receptor subtypes (18). However, no significant pharmacological differences were reported between homo- and heterodimers for these closely related 5-HT receptor subtypes. Recently, a study identified other 5-HT receptor heterodimers with functional implication; heterodimers between 5-HT$_{1A}$ and 5-HT$_7$ receptors have been reported to regulate GIRK channel activity in heterologous systems and in hippocampal neurons (29). Heterodimerization was found to inhibit 5-HT$_{1A}$-mediated activation of Gα_i and GIRK channel activity, without affecting 5-HT$_7$ receptor-mediated signaling, indicating a unidirectional dominant effect of the 5-HT$_7$ protomer. Of note, cross-talks between 5-HT receptors have been reported without obligatory physical interaction. For instance, co-expression of the 5-HT$_{1B}$ and 5-HT$_{2B}$ receptors influences the internalization pathways and kinetics of both receptors without heterodimerization (*i.e.* lack of FRET signal) (30).

To date, neither the basic pharmacological profiles of putative 5-HT$_2$ heterodimers nor their signaling properties have been characterized. We specifically addressed this issue here by studying the interactions between the three members of the 5-HT$_2$ subfamily and their functional consequences *in vitro* and *in vivo*. Using co-immunoprecipitation and bioluminescence resonance energy transfer (BRET) approaches, we found that 5-HT$_{2A}$, 5-HT$_{2B}$, and 5-HT$_{2C}$ form heterodimers when co-expressed in heterologous expression systems. Although 5-HT$_{2C}$-containing heterodimers did not show alterations in coupling properties, the signaling of associated 5-HT$_{2A}$ or 5-HT$_{2B}$ protomers was blunted, whereas the 5-HT$_{2C}$ protomer maintained its signaling properties. Moreover, no blunting occurred in 5-HT$_{2A/2B}$ heterodimers. We next showed that this asymmetry in Gα_q protein activation was related to a dominant effect of the 5-HT$_{2C}$ protomer on ligand binding to the other partner. Using AAV-mediated exogenous expression of a 5-HT$_{2C}$ receptor-truncated C-tail mutant (5-HT$_{2C\Delta Cter}$) in brain regions expressing endogenous 5-HT$_{2A}$ receptor, we also observed a blunting effect of this inactive 5-HT$_{2C}$ receptor leading to a complete binding inhibition of the 5-HT$_{2A}$-selective ligand. Accordingly, this lack of ligand binding was associated with impaired 5-HT$_{2A}$-induced excitatory neurotransmission in neurons expressing the 5-HT$_{2C}$-inactive protomer.

Results

Interactions between 5-HT$_2$ receptors

The putative formation of heterodimers between 5-HT$_2$ receptor subtypes was investigated using BRET and co-immunoprecipitation experiments (Fig. 1). The coding region of *Renilla* luciferase (Rluc, BRET donor) or the yellow variant of the green fluorescent protein (YFP, BRET acceptor), were fused in-phase downstream of the coding region of 5-HT$_{2A}$, 5-HT$_{2B}$, and 5-HT$_{2C}$ receptors. Saturation BRET experiments were conducted in HEK293 cells co-transfected with constant amounts of BRET donor plasmids and increasing amounts of BRET acceptor plasmids. In case of a close proximity between the investigated partners, hyperbolic saturation of the BRET signal is expected (see under "Experimental procedures"). Hyperbolic curves were indeed obtained when 5-HT$_{2A}$ or 5-HT$_{2C}$ receptors were tested for self-association (5-HT$_{2A/2A}$ and 5-HT$_{2C/2C}$, respectively, Fig. 1*a*), confirming previous studies showing that these receptors are able to homodimerize in transfected cells (13, 14). Noteworthy, the same experiment with 5-HT$_{2B}$ BRET pairs led to a linear plot, consistent with a bystander (nonspecific) BRET and thus with the absence of self-association. Hyperbolic curves were also obtained with 5-HT$_{2A}$ and 5-HT$_{2C}$ BRET pairs (5-HT$_{2A/2C}$), 5-HT$_{2B}$ and 5-HT$_{2C}$ BRET pairs (5-HT$_{2B/2C}$), and 5-HT$_{2A}$ and 5-HT$_{2B}$ (5-HT$_{2A/2B}$) BRET pairs (Fig. 1*b*), suggesting that 5-HT$_2$ receptors can form heterodimers in intact cells. BRET$_{50}$ values (values of YFP/Rluc for half-maximal BRET) reflect the propensity of association between the investigated proteins. Interestingly, BRET$_{50}$ values for heterodimeric association are significantly lower than those measured for homodimeric association of 5-HT$_2$ subtypes, suggesting that in native cells expressing more than one 5-HT$_2$ receptor subtype heterodimerization is favored over homodimerization (Fig. 1*b*).

The physical interaction between these receptor subtypes was confirmed by co-immunoprecipitation studies in the same cells, using epitope (FLAG)- or GFP-tagged proteins (Fig. 1*c*). Consistent with BRET data, FLAG-5-HT$_{2C}$ receptor co-immunoprecipitated with 5-HT$_{2A}$-GFP and 5-HT$_{2C}$-GFP receptors. In complementary experiments FLAG-5-HT$_{2B}$ receptor co-immunoprecipitated with 5-HT$_{2A}$-GFP and 5-HT$_{2C}$-GFP receptors.

Impact of dimerization of 5-HT$_2$ receptors on signaling

We next examined the consequence of 5-HT$_2$-receptor heterodimerization on agonist-induced Gα_q activation. The 5-HT$_2$ receptors consistently activate the PLC-β pathway in native tissues and heterologous cells (3, 12). We first determined whether 5-HT$_2$ receptor signaling was altered when expressed in the presence of other 5-HT$_2$ receptors (Fig. 2). Dose-response curves of 5-HT$_2$-mediated production of IP in response to 5-HT or the partial agonist DOI in cells expressing 5-HT$_{2A}$, 5-HT$_{2B}$, or 5-HT$_{2C}$ receptors and in combination were analyzed using the operational model (31) to determine the Gα_q coupling efficiency of single receptors and heterodimers (Fig. 2). No significant difference in Gα_q coupling efficiency as determined by the transduction coefficient (τ/K_A) (32) was found among the groups, supporting a lack of major difference

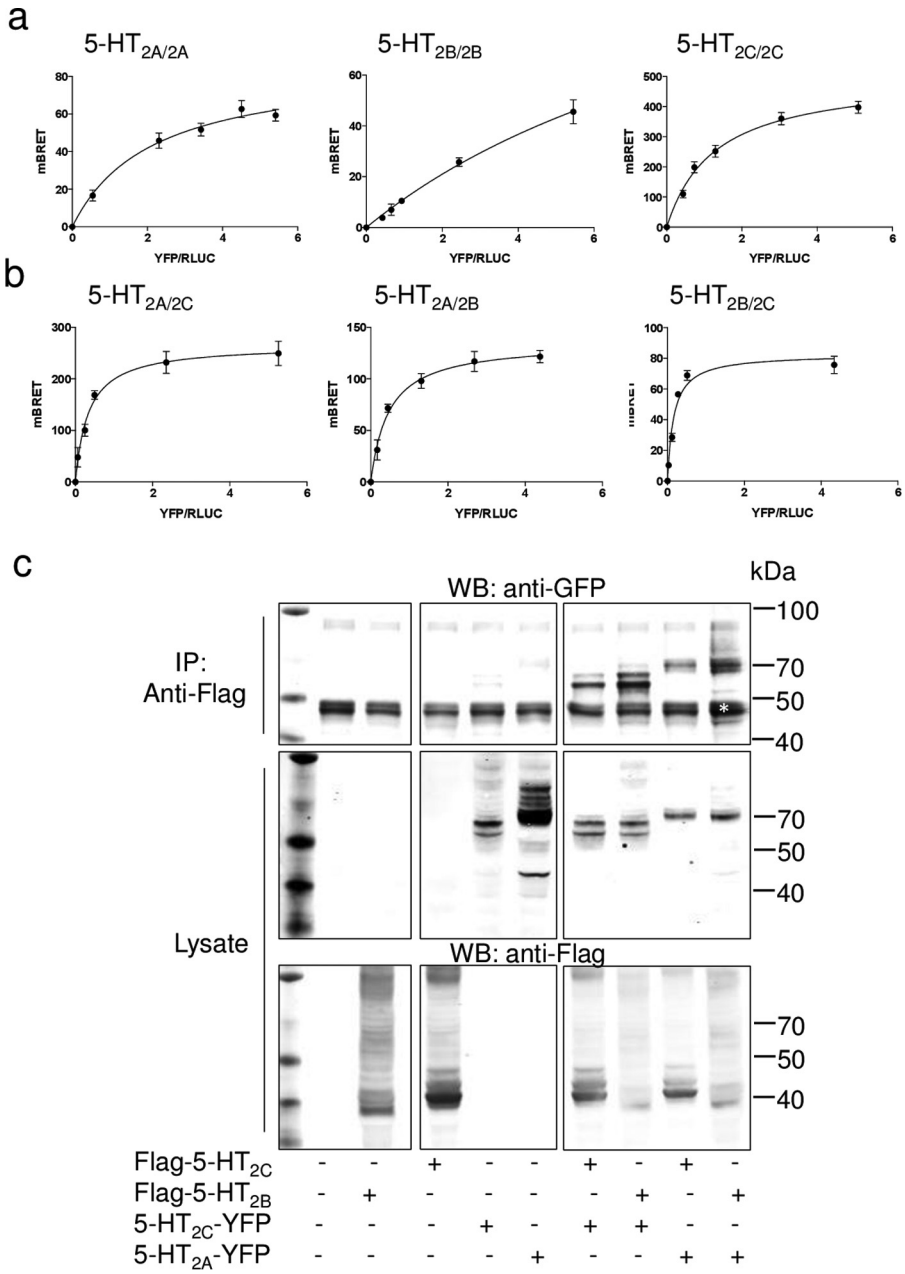

Figure 1. Constitutive heterodimerization of 5-HT$_2$ receptors and co-immunoprecipitation in living HEK293 cells. *a,* BRET proximity assays between homodimers of 5-HT$_{2A}$, 5-HT$_{2B}$, or 5-HT$_{2C}$ receptors. HEK293 cells were co-transfected with plasmids coding for a constant amount of RLuc-5-HT$_{2A}$, RLuc-5-HT$_{2B}$ or RLuc-5-HT$_{2C}$ (BRET donors) and increasing concentrations of the corresponding YFP tagged 5-HT$_2$ homodimer (the BRET acceptor). *b,* BRET proximity assays between heterodimers of 5-HT$_{2A}$, 5-HT$_{2B}$, or 5-HT$_{2C}$ receptors. HEK293 cells were co-transfected with plasmids coding for a constant amount of RLuc-5-HT$_{2A}$, RLuc-5-HT$_{2B}$, or RLuc-5-HT$_{2C}$ (BRET donors) and increasing concentrations of YFP-tagged 5-HT$_2$ heterodimer (the BRET acceptor). For each heterodimers, BRET donor and acceptor were swapped as a control experiment (data not shown). Energy transfer was measured after addition of membrane-permeable luciferase substrate coelenterazine-h. The BRET signal was determined by calculating the ratio of light emitted at 530 nm and that emitted at 485 nm, as described under "Experimental procedures." *Error bars* indicate S.E. of specific BRET-ratio values obtained from triplicate determinations. BRET values (B_{max}, BRET$_{50}$) were obtained from six independent experiments. Plots were established using GraphPad software. 5-HT$_{2A/2A}$: BRET$_{max}$ 76 $\pm$ 16, BRET$_{50}$ 2.4 $\pm$ 0.5; 5-HT$_{2B/2B}$ ambiguous: 5-HT$_{2C/2C}$: BRET$_{max}$ 434 $\pm$ 32, BRET$_{50}$ 1.2 $\pm$ 0.4; 5-HT$_{2A/2C}$: BRET$_{max}$ 266 $\pm$ 24, BRET$_{50}$ 0.33 $\pm$ 0.04; 5-HT$_{2A/2B}$: BRET$_{max}$ 90 $\pm$ 32, BRET$_{50}$ 0.19 $\pm$ 0.07; 5-HT$_{2B/2C}$: BRET$_{max}$ 85 $\pm$ 6, BRET$_{50}$ 0.16 $\pm$ 0.04. *c,* interactions of 5-HT$_2$ subtypes in co-immunoprecipitation experiments. COS-7 cells were transfected with various combinations of plasmids coding for 5-HT$_{2A}$-YFP, 5-HT$_{2C}$-YFP, and FLAG epitope-tagged 5-HT$_{2B}$ and 5-HT$_{2C}$, as indicated. Immunoprecipitation with a monoclonal anti-FLAG antibody-coated beads (EZview Red FLAG M2 affinity gel) was performed from 1 mg of protein of cell lysates. The presence of 5-HT$_2$-GFP and 5-HT$_2$-FLAG was revealed with anti-GFP and anti-FLAG antibodies, respectively. 100 μg of protein of cell lysates were analyzed to determine receptor-GFP receptor-FLAG expression (input). *White asterisk,* IgG heavy chain. *WB*, Western blotting; *IP*, immunoprecipitation.

in coupling efficiency between individual 5-HT$_2$ receptors to Gα_q activation and no modification of this coupling efficiency by heterodimers.

In the absence of highly selective, subtype-specific 5-HT$_2$ agonists, we next determined whether agonist-induced 5-HT$_2$ heterodimer signaling was altered in the presence of selective antagonist of the other protomer (Fig. 5). Affinity and selectivity of antagonists were first tested in transfected cells to define the optimal concentration that nearly fully inhibits each individual receptor and to avoid cross-reactivity (100 nM, Fig. 3).

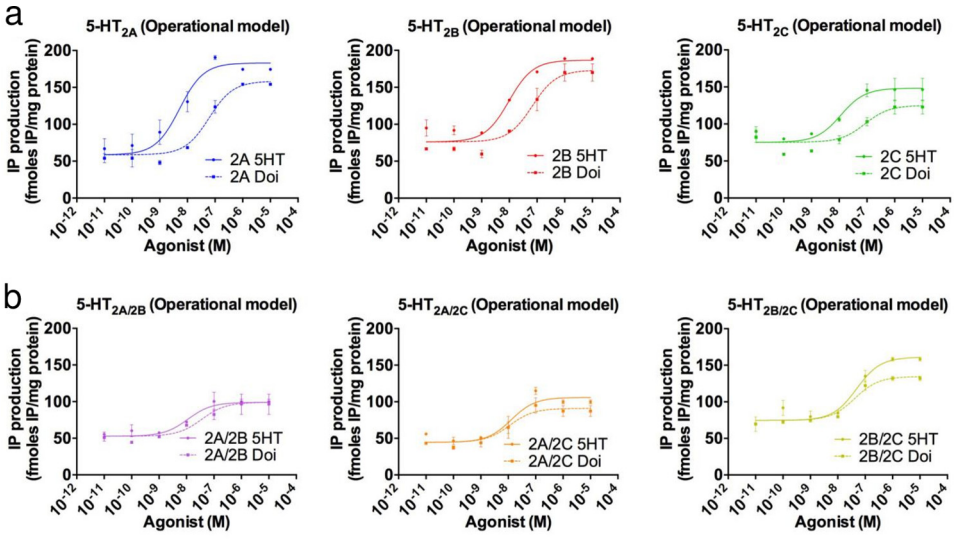

c

Log (τ/K_A)	5-HT$_{2A}$	5-HT$_{2B}$	5-HT$_{2C}$	5-HT$_{2A/2B}$	5-HT$_{2A/2C}$	5-HT$_{2B/2C}$
	-7.11±0.31	-7.58±0.19	-6.69±0.22	-7.30±0.20	-7.26±0.38	-7.22±0.19

Figure 2. IP production induced by stimulation by a full (5-HT) and a partial agonist (DOI). *a,* 5-HT and DOI dose-response curves in single receptor transfections. COS-7 cells transiently expressing 5-HT$_{2A}$, 5-HT$_{2B}$, 5-HT$_{2C}$, and receptor alone, were stimulated with serotonin (5-HT) or DOI, and IP levels were determined. For each condition, stimulation with 5-HT induces full dose-response curve and DOI a partial dose response that can be modelized using the operational model. *b,* 5-HT and DOI dose-response curves in two receptor transfections. COS-7 cells transiently co-expressing 5-HT$_{2A/2B}$, 5-HT$_{2A/2C}$, and 5-HT$_{2B/2C}$ receptors were stimulated with serotonin (5-HT), or DOI and IP levels were determined. These are representative curves of at least four independent experiments performed in duplicate. *c,* dose-response curves allow us to calculate the mean log(τ/K_A), which is not affected by dimerization (one-way ANOVA, $n = 4–5$). Values are given ± S.E.

Dose-response curves of 5-HT$_2$-mediated IP accumulation in response to 5-HT stimulation allowed the determination of the minimal agonist concentration inducing maximal IP response (1 μM, Fig. 4*a*). When expressed individually, 5-HT$_2$ receptors displayed significant 5-HT-stimulated IP production (Fig. 5*a*); in the presence of selective antagonists (MDL100970 for 5-HT$_{2A}$, RS127445 for 5-HT$_{2B}$, and RS102221 for 5-HT$_{2C}$ receptors), the agonist-stimulated IP response was reduced to basal level in cells expressing the cognate 5-HT$_2$ receptor (Fig. 5*a*).

In the 5-HT$_{2A/2B}$ heterodimers, the 5-HT$_{2A}$ receptor contributed to the activation of the Gα_q/PLC-β pathway in response to agonist, as demonstrated by the inhibitory effect of MDL100907 (Fig. 5*a*); reciprocally, the 5-HT$_{2B}$ receptor was also contributing to signaling when co-expressed with 5-HT$_{2A}$ receptors, as demonstrated by the inhibitory effect of RS127445 (Fig. 5*a*). By contrast in the 5-HT$_{2B/2C}$ heterodimers, only the 5-HT$_{2C}$ receptors continued mediating signaling, because blocking selectively the 5-HT$_{2B}$ receptors with RS127445 did not inhibit the 5-HT-mediated IP accumulation (Fig. 5*a*), although it can be blocked only by selective 5-HT$_{2C}$ receptor antagonists RS102221 or SB242084 (Figs. 5*a* and 4, *c* and *d*). The 5-HT$_{2A}$-mediated IP accumulation was similarly blunted by expression of the 5-HT$_{2C}$ receptor, as MDL100907 had no significant inhibitory effect on IP production but RS102221 did (Fig. 5*a*).

The same effect was reproduced for different agonists 5-HT or nor-(+)-fenfluramine (NDF) (Fig. 4, *e* and *f*) and in all tested cell lines, COS-7 (Fig. 2), HEK293 (Figs. 4–5), CHO (Fig. 6*c*), or LMTK (Fig. 6, *a* and *b*), and thus is likely independent of agonists or cell-specific effectors. Because it was shown above that under the same expression conditions these receptor isoforms constitute heterodimers, a plausible explanation for the observed effects is that heterodimerization with 5-HT$_{2C}$ prevents the ability of 5-HT$_{2A}$ or 5-HT$_{2B}$ receptors to signal, whereas in the case of heterodimerization of 5-HT$_{2A}$ with 5-HT$_{2B}$ receptors, both 5-HT$_{2A}$ and 5-HT$_{2B}$ protomers contribute to signal.

These results are consistent with a model where in the 5-HT$_{2A/2C}$ and 5-HT$_{2B/2C}$ heterodimers, only the 5-HT$_{2C}$ protomer couples to the G protein, while preventing coupling of the associated protomer. To investigate this issue, we co-expressed the 5-HT$_{2A}$ or 5-HT$_{2B}$ receptor with a 5-HT$_{2C}$ receptor deleted for the C-terminal tail (5-HT$_{2C\Delta Cter}$) (Fig. 5*b*), a mutant receptor incapable of activating Gα_q and stimulating IP production in response to 5-HT stimulation (Fig. 5*b*). Confirming the hypothesis, in cells expressing 5-HT$_{2A/2C\Delta Cter}$ and 5-HT$_{2B/2C\Delta Cter}$ heterodimers, IP accumulation was dramatically reduced (Fig. 5*b*). In addition, co-expressing 5-HT$_{2C}$ receptors with 5-HT$_{2B\Delta Cter}$, a 5-HT$_{2B}$ receptor similarly deleted for the C-terminal tail and impaired for IP accumulation, had no impact on 5-HT$_{2C}$ signaling (Fig. 5*b*) because it was still sensitive to RS102221, supporting that only the 5-HT$_{2C}$ protomer couples to the G$_q$ protein. We confirmed the proper plasma membrane expression of the 5-HT$_{2C\Delta Cter}$ and 5-HT$_{2B\Delta Cter}$ receptor constructs compared with the respective WT form, using a radioligand binding assay on non-permeabilized cells. Expression of 5-HT$_{2B}$, 5-HT$_{2B\Delta Cter}$, 5-HT$_{2C}$, or 5-HT$_{2C\Delta Cter}$ receptors in HEK cells leads to 37, 50, 20, and 53% of construct surface expression compared with total whole cell membrane expression (permeabilized cells), respectively, suggesting that ΔCter constructs are expressed properly at the cell membrane. Moreover, BRET assay confirms the ability of the two ΔCter

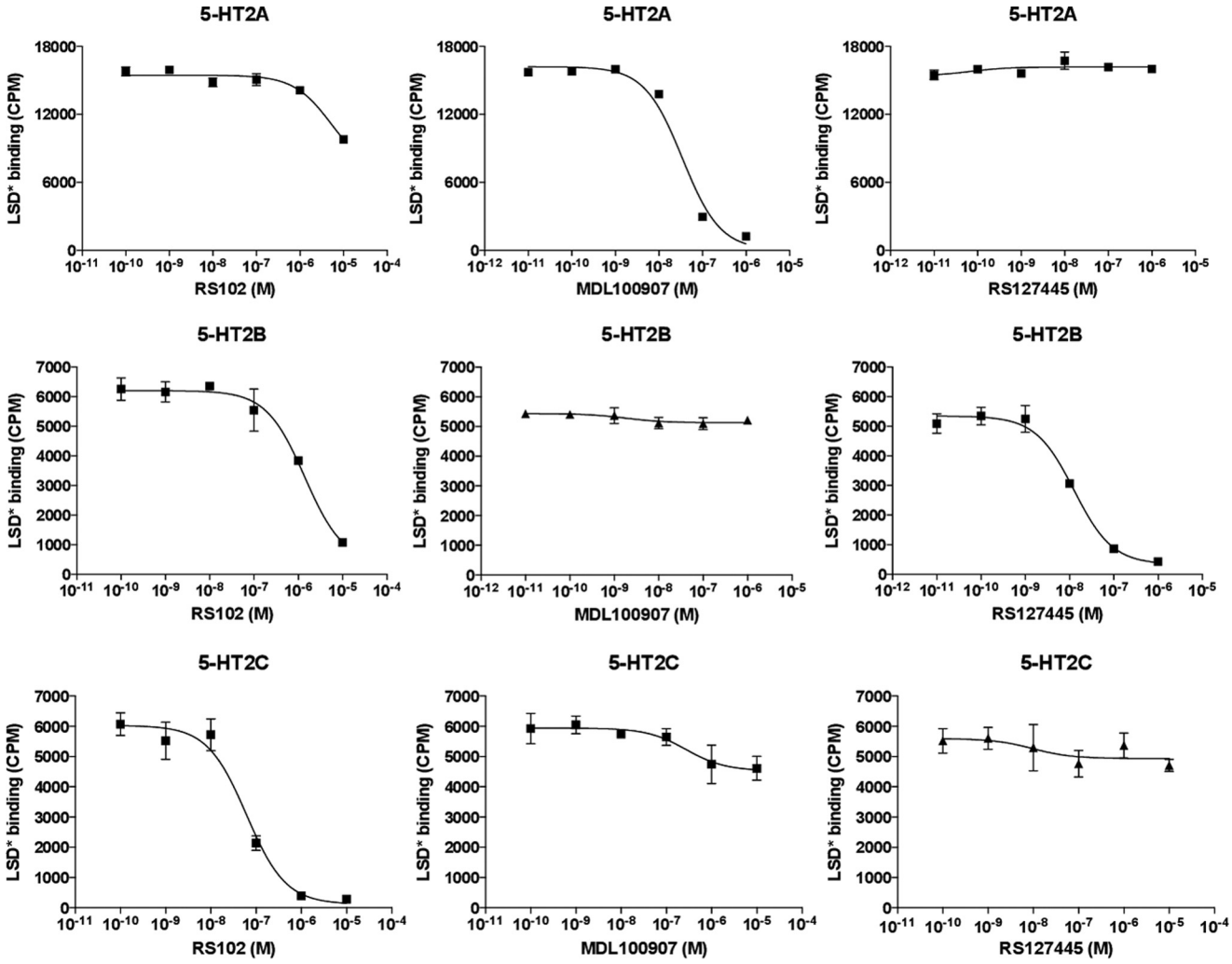

Figure 3. Affinity and selectivity of antagonists used in this study. Affinity and selectivity of antagonists were tested to define the optimal concentration and avoid cross-reactivity. Representative examples of [^{3}H]LSD radioligand binding heterologous competition experiments performed on membrane preparations are shown. HEK293 cells transiently expressing 5-HT$_{2A}$, 5-HT$_{2B}$, or 5-HT$_{2C}$ receptors were incubated with [^{3}H]LSD and increasing concentrations of the 5-HT$_{2A}$ (MDL100907), 5-HT$_{2B}$ (RS127445), and 5-HT$_{2C}$ (RS102221) antagonist. Thus, we used in this study 100 nM concentration for all the antagonists. *Graphs* are representative of one experiment performed in triplicate. *Bars* represent ± S.E. from triplicates. Binding curves were done using GraphPad software.

constructs to associate with 5-HT$_{2A}$, 5-HT$_{2B}$, or 5-HT$_{2C}$ protomers (Fig. 7, *a–d*). To confirm these findings, in cell expressing constant 5-HT$_{2B}$ and variable amounts of 5-HT$_{2C}$ receptors, the progressive decrease of 5-HT$_{2C}$ expression level allowed the recovery of 5-HT$_{2B}$ receptor-dependent signaling (the fraction of IP accumulation inhibited by the 5-HT$_{2B}$-selective RS127445), likely due to reduced formation of 5-HT$_{2B/2C}$ heterodimers (Fig. 7*e*).

Impact of dimerization on 5-HT$_2$ receptor-binding properties

The results above are thus consistent with a model where in the 5-HT$_{2A/2C}$ and 5-HT$_{2B/2C}$ heterodimers, only the 5-HT$_{2C}$ protomer couples to the G$_q$ protein, while preventing ligand binding of the associated protomer. To examine this hypothesis, agonist (5-[^{3}H]HT or [^{3}H]LSD) radioligand binding assays were conducted in the presence or absence of the 5-HT$_{2C}$ receptor and of increasing concentrations of selective antagonists (MDL100907 for 5-HT$_{2A}$, RS127445 for 5-HT$_{2B}$, and RS102221 for 5-HT$_{2C}$) in cells expressing similar quantities of receptors (Fig. 8). RS127445 could compete for 5-[^{3}H]HT (Fig. 8*a*) or [^{3}H]LSD (Fig. 8*c*) binding in cells only expressing 5-HT$_{2B}$ receptors, whereas no competition was observed in cells expressing 5-HT$_{2B/2C}$ receptors. In contrast, RS102221 could displace 5-[^{3}H]HT (Fig. 8*b*) or [^{3}H]LSD (Fig. 8*d*) binding in cells expressing either 5-HT$_{2C}$ receptors alone or 5-HT$_{2B}$/$_{2C}$ receptors. Similar findings were obtained for 5-HT$_{2A}$ receptors (Fig. 8, *e* and *f*). Noteworthy, 5-[^{3}H]HT or [^{3}H]LSD binding was comparable in cells expressing 5-HT$_{2C}$ alone or 5-HT$_{2C}$ receptor and another 5-HT$_2$ isoform, indicating that the presence of 5-HT$_{2C}$ receptors almost completely inhibits ligand binding to co-expressed 5-HT$_{2A}$ and 5-HT$_{2B}$ receptors. Strictly similar findings were observed with the 5-HT$_{2B\Delta Cter}$ receptor (Fig. 8, *g* and *h*) or with radiolabeled antagonist ([^{3}H]mesulergine) binding experiments (Fig. 8, *i–k*) supporting that 5-HT$_{2C}$ protomers somehow masked the ligand-binding site of the other protomer in 5-HT$_2$ heterodimers, independently of the coupling ability of the complex.

A possibility is that the presence of a 5-HT$_{2C}$ protomer is sufficient to compete with plasma membrane accessibility of either 5-HT$_{2A}$ or 5-HT$_{2B}$ protomers. Surface expression of

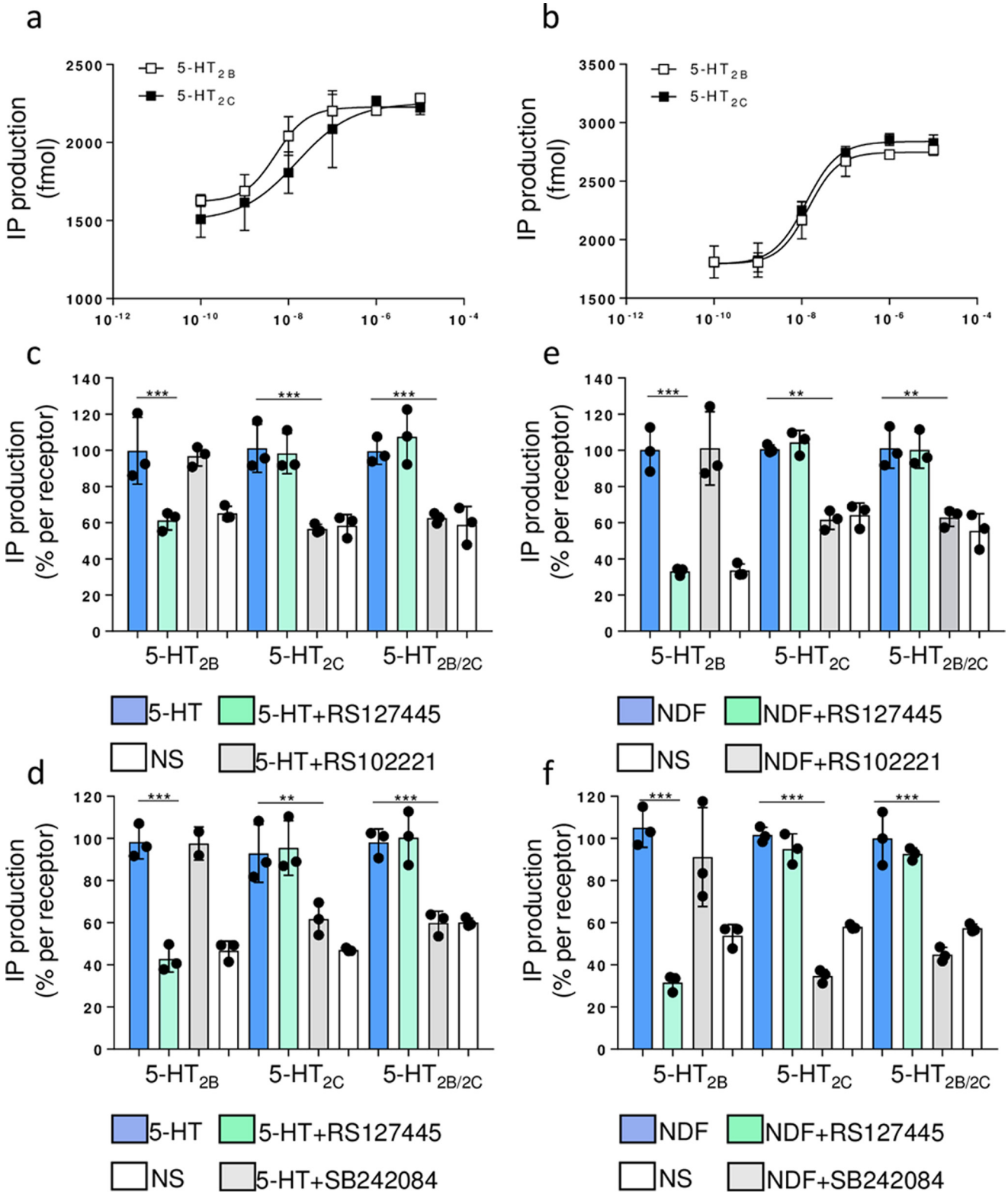

Figure 4. 5-HT$_{2C}$ receptor expression blocks 5-HT$_{2B}$ receptor signaling. *a, b,* agonist concentration-induced IP response. *a,* serotonin (5-HT) (*a*) and NDF (*b*) dose-response curves for stimulation of IP production in cells expressing the same amount of 5-HT$_{2B}$ (*white box*) or 5-HT$_{2C}$ (*dark box*) receptors were used to obtain the minimal agonist concentration-induced maximal IP response (1 μM for both agonists). *Bars* represent ± S.E. from triplicates. *c–f,* HEK293 cells transiently expressing 5-HT$_{2C}$ and 5-HT$_{2B}$ receptor alone or in combination (5-HT$_{2B/2C}$) were stimulated with 1 μM 5-HT$_2$ agonist serotonin (5-HT) or NDF, and IP accumulation was determined. The selective 5-HT$_{2B}$ (RS127445, *green*) or 5-HT$_{2C}$ antagonists RS102221 (*gray*) or SB242084 (*gray*) were co-incubated with agonists. Data are expressed as % of agonist response for each transfected condition. *Bars* represent ± S.D. of three independent experiments. *NS,* non-stimulated. Data were analyzed with one-way ANOVA within each independent transfection and a Bonferroni's multiple comparisons test. ***, $p < 0.005$; **, $p < 0.01$. Specific antagonist treatments were significantly different from 5-HT stimulation.

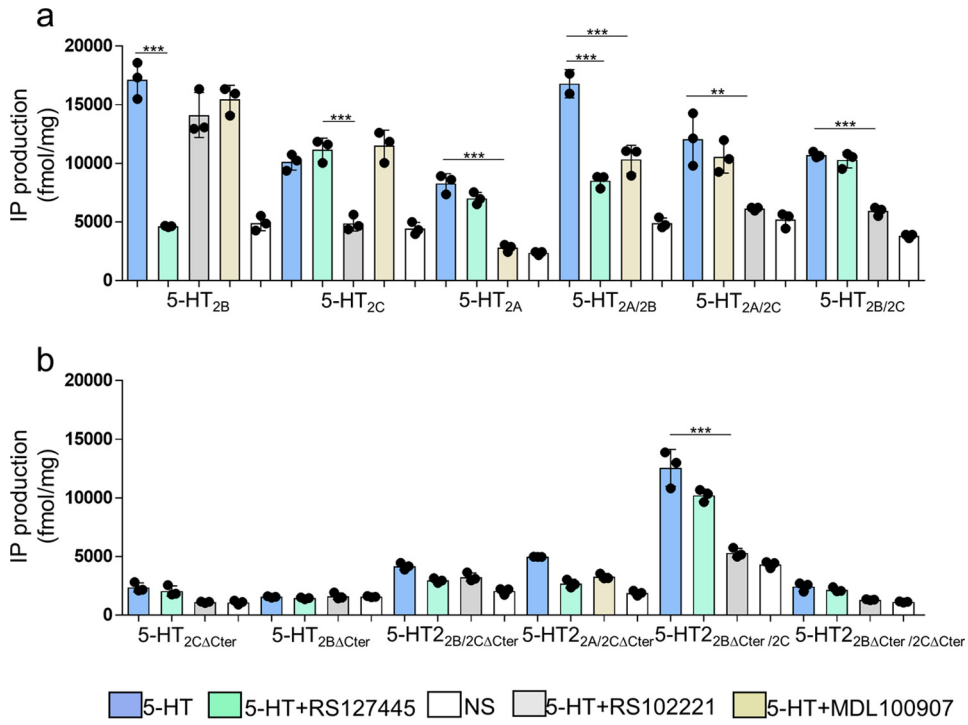

Figure 5. 5-HT$_{2C}$ receptor blunts 5-HT$_{2A}$ and 5-HT$_{2B}$ receptor signaling. HEK293 cells transiently expressing 5-HT$_{2A}$, 5-HT$_{2B}$, 5-HT$_{2C}$, 5-HT$_{2B\Delta Cter}$, and 5-HT$_{2C\Delta Cter}$ receptor, alone or in combination, were stimulated with 1 μM serotonin (5-HT), and IP levels were determined. The selective antagonists (100 nM), 5-HT$_{2B}$ (*green*, RS127445), 5-HT$_{2C}$ (*gray*, RS102221), or 5-HT$_{2A}$ (*brown*, MDL100907) were co-incubated with 5-HT as indicated. *a*, compared with receptors alone, which produce IP accumulation that can be blocked by the respective selective antagonists, IP accumulation can only be blocked by 5-HT$_{2C}$ receptor antagonist but not the 5-HT$_{2A}$ or 5-HT$_{2B}$ receptor antagonist in co-transfection of either 5-HT$_{2A}$ or 5-HT$_{2B}$ with 5-HT$_{2C}$ receptors. *b*, stimulation of 5-HT$_{2B\Delta Cter}$, 5-HT$_{2C\Delta Cter}$, or HT$_{2B\Delta Cter/2C\Delta Cter}$ receptors gives little IP accumulation. Stimulation of 5-HT$_{2A/2C\Delta Cter}$ or HT$_{2B/2C\Delta Cter}$ receptors gives also nearly no IP accumulation, whereas 5-HT$_{2C/2B\Delta Cter}$ leads to IP accumulation that can only be blocked by the 5-HT$_{2C}$ receptor antagonist. *Bars* represent $\pm$ S.D. of three independent experiments. *NS*, non-stimulated. Data were analyzed with one-way ANOVA within each independent transfection and a Bonferroni's multiple comparisons test. ***, $p < 0.005$; **, $p < 0.01$. Specific antagonist treatments are significantly different from 5-HT stimulation.

both receptors was measured by cytometry using a Pacific Blue-conjugated antibody directed against extracellular 3×FLAG-tagged 5-HT$_2$-YFP constructs, with YFP being intracellular and reflecting total expression of the receptor (Fig. 9). The ratio of cell-surface receptors over the total obtained (mean of Pacific Blue signal/mean of GFP) for each condition was normalized as the percentage of 5-HT$_{2A}$ (Fig. 9, *a* and *b*) or 5-HT$_{2B}$ receptor alone. 5-HT$_{2A}$ (Fig. 9*c*) or 5-HT$_{2B}$ (Fig. 9*d*) receptors in cells co-transfected with 5-HT$_{2C}$ receptors were not significantly different compared with control (single expression), although co-expression of 5-HT$_{2A}$ receptors slightly increased cell-surface expression of 5-HT$_{2B}$ receptors. Decreased ligand binding or Gα_q coupling of 5-HT$_{2A}$ or 5-HT$_{2B}$ receptors co-expressed with 5-HT$_{2C}$ receptor cannot be explained by reduced cell-surface expression.

Heterodimer properties in vivo

The inhibitory role of 5-HT$_{2C}$ on 5-HT$_{2A}$ and 5-HT$_{2B}$ receptor binding and coupling was next analyzed in neurons. Mouse prefrontal cortex (PFC) neurons, which have been shown to express 5-HT$_{2A}$ receptors (33, 34), were used as a model system. Accordingly, exogenous 5-HT$_{2C\Delta Cter}$ expression in PFC, upon infection with adeno-associated viruses carrying a 5-HT$_{2C\Delta Cter}$ construct (AAV-5-HT$_{2C\Delta Cter}$), was associated with an increase of [^{3}H]mesulergine able to bind to endogenous 5-HT$_{2A}$ and exogenous 5-HT$_{2C\Delta Cter}$ receptors (Fig. 10*a*). However, a dramatic inhibition of endogenous 5-HT$_{2A}$ receptor-dependent ligand binding compared with AAV-mediated GFP expression was also observed (absence of MDL100907-induced [^{3}H]mesulergine displacement) (Fig. 10*a*). We then investigated whether the 5-HT$_{2C}$ receptor was also able to suppress 5-HT$_{2A}$ receptor-dependent signaling *in vivo* via heterodimerization. We thus used the same adenoviral delivery system to express the inactive 5-HT$_{2C\Delta Cter}$ protomer in adrenergic locus ceruleus (LC) neurons. Previous studies reported that the 5-HT$_2$ receptor agonist DOI decreases the firing rate of 5-HT neurons in the dorsal raphe (DR) nucleus (35, 36). This inhibitory response was completely blunted in 5-*Htr*$_{2A}^{-/-}$ mice and was attenuated (30%) by inducing the loss of noradrenergic neurons with the DSP4 neurotoxin (37). Indeed, activation by DOI of 5-HT$_{2A}$ receptors expressed on GABAergic interneurons of the LC (38, 39) decreased noradrenergic tone thereby limiting its excitatory influence on DR 5-HT neurons. A corollary of these functional interactions between monoaminergic neurons is a significant decrease of DR 5-HT neuronal activity. We then used this paradigm as a functional read-out for norepinephrine transmission upon expression of the functionally inactive 5-HT$_{2C\Delta Cter}$ protomer (Fig. 10, *b–d*). Bilateral stereotaxic injections of AAV-5-HT$_{2C\Delta Cter}$ IRES GFP or AAV GFP in the LC were performed 1 month before *in vivo* electrophysiological recordings of DR 5-HT neurons (Fig. 10*b*). Mouse brains samples were examined to verify the distribution of adenovirus-encoded 5-HT$_{2C\Delta Cter}$ and GFP in the LC (Fig. 10*c*). In mice injected with

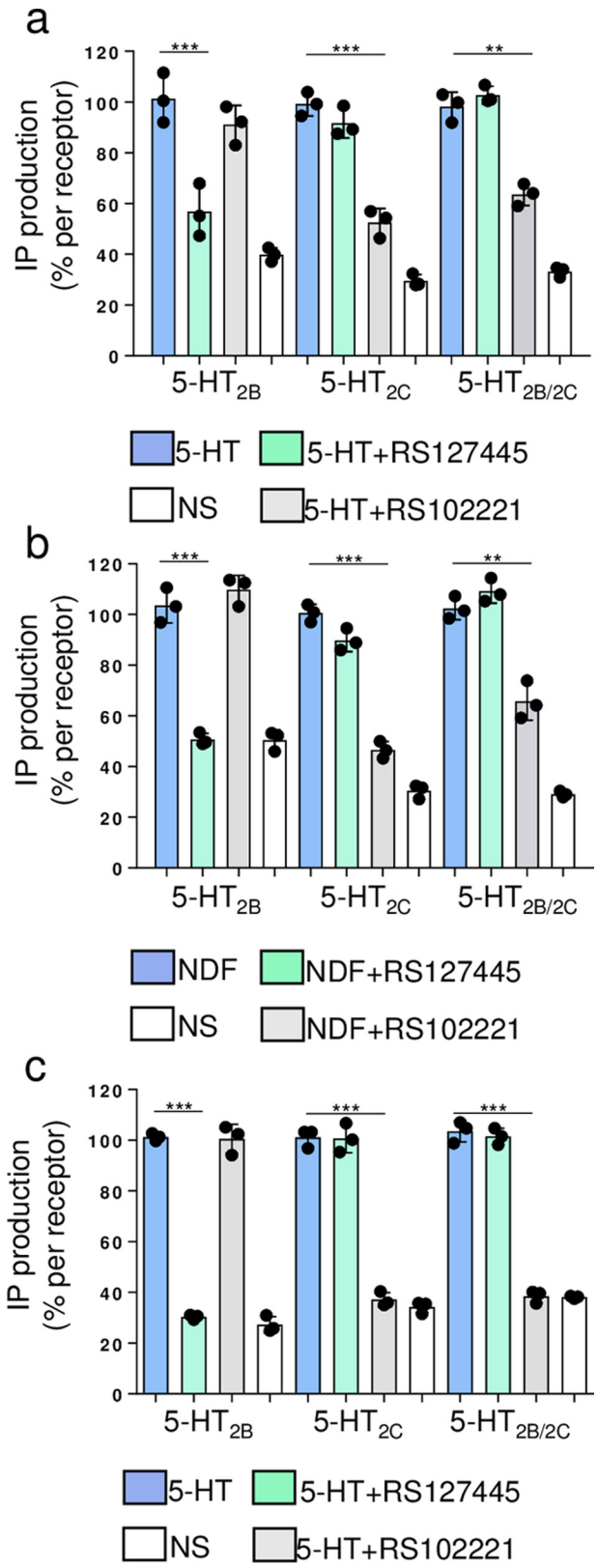

Figure 6. 5-HT$_{2C}$ receptor blunts 5-HT$_{2B}$ receptor signaling independently of the cell types. LMTK$^-$ (*a* and *b*) or CHO (*c*) cells transiently expressing 5-HT$_{2C}$ and 5-HT$_{2B}$ receptor alone or in combination (5-HT$_{2B/2C}$) were stimulated with 1 μM of the 5-HT$_2$ agonist serotonin (*5-HT*) or NDF, and IP accumulation was determined. The selective 5-HT$_{2B}$ (RS127445, *green*) or 5-HT$_{2C}$ antagonists (RS102221, *gray*) were co-incubated with agonist in some conditions, as indicated. Data are expressed as % of maximal agonist response for each transfected condition. *Bars* represent ± S.D. of three independent experiments. *NS*, non-stimulated. Data were analyzed with one-way ANOVA for each graph and a Bonferroni's multiple comparisons test. ***, $p < 0.005$; **, $p < 0.01$. Specific antagonist treatments are significantly different from 5-HT stimulation.

control AAV (AAV GFP), increasing DOI concentrations induced a progressive decrease of the firing rate of DR 5-HT neurons (Fig. 10*d*), as observed by previous reports (37). This inhibitory response was strongly reduced (50%) in AAV-5-HT$_{2C\Delta Cter}$-injected mice (Fig. 10*d*), consistent with an impaired signaling of 5-HT$_{2A}$ receptors. These data indicate that 5-HT$_{2C\Delta Cter}$ receptors inhibit 5-HT$_{2A}$ receptor-mediated signaling in neurons, likely via their heterodimerization with 5-HT$_{2A}$ receptors.

Discussion

Our data demonstrate that 5-HT$_{2A}$, 5-HT$_{2B}$, and 5-HT$_{2C}$ receptors heterodimers are favored and able to form *in vitro* and *in vivo*. Although heterodimerization with 5-HT$_{2C}$ receptors does not apparently modify the coupling ability to the Gα_q pathway, it appears to blunt binding properties of 5-HT$_{2A}$ and 5-HT$_{2B}$ protomers. These findings can be interpreted as uni-directional dominance of 5-HT$_{2C}$ over the two other protomers in 5-HT$_{2A/2C}$ and 5-HT$_{2B/2C}$ heterodimers. The masking effect exerted by the 5-HT$_{2C}$ protomer is specific, because no similar functional consequences could be observed in 5-HT$_{2A/2B}$ heterodimers. This dominance appears to be independent of ligands (agonists or antagonists), of the cell type or of the plasma membrane accessibility of the different protomers.

Uni-directional activating or inhibiting effects of protomers on ligand binding or coupling properties of the cognate partner were reported for few GPCR heterodimers (40). For example, G protein coupling of angiotensin AT1 receptor is inhibited in AT1/AT2 or AT1/APJ (the receptor for apelin) heterodimers (41, 42) but not in AT1/5-HT$_{2B}$ heterodimers (28). In this context, impaired coupling can be caused by different mechanisms. Ligand occupancy of one protomer of the heterodimer can induce conformational changes of the binding pocket of the second protomer resulting in ligand binding inhibition (43). The inhibitory effect of one protomer can also occur in the absence of its ligand. For example, the long C-terminal tail of the orphan receptor GPR50 indirectly prevents the binding of melatonin to the MT1 melatonin receptor in GPR50-MT1 heterodimers (44).

Here, we show that 5-HT$_{2C\Delta Cter}$, which lacks the capacity of activating Gα_q proteins, inhibits both Gα_q coupling and ligand binding of associated 5-HT$_2$ protomers. These data indicate that asymmetric "sequestration" of Gα_q by the C-terminal tail of the 5-HT$_{2C}$ receptor does not account for the observed effect. Consistent with previous observations, showing that a 5-HT$_2$ protomer can promote conformational changes across asymmetrical dimer interface (45, 46), 5-HT$_{2C}$-dependent inhibition of 5-HT$_{2A}$ and 5-HT$_{2B}$ protomer binding might occur via a similar mechanism.

Interestingly, when 5-HT$_{2C}$ receptors were co-expressed with 5-HT$_{2A}$ or 5-HT$_{2B}$ receptors, binding and functional studies indicated the absence of 5-HT$_{2A}$- or 5-HT$_{2B}$-dependent sig-

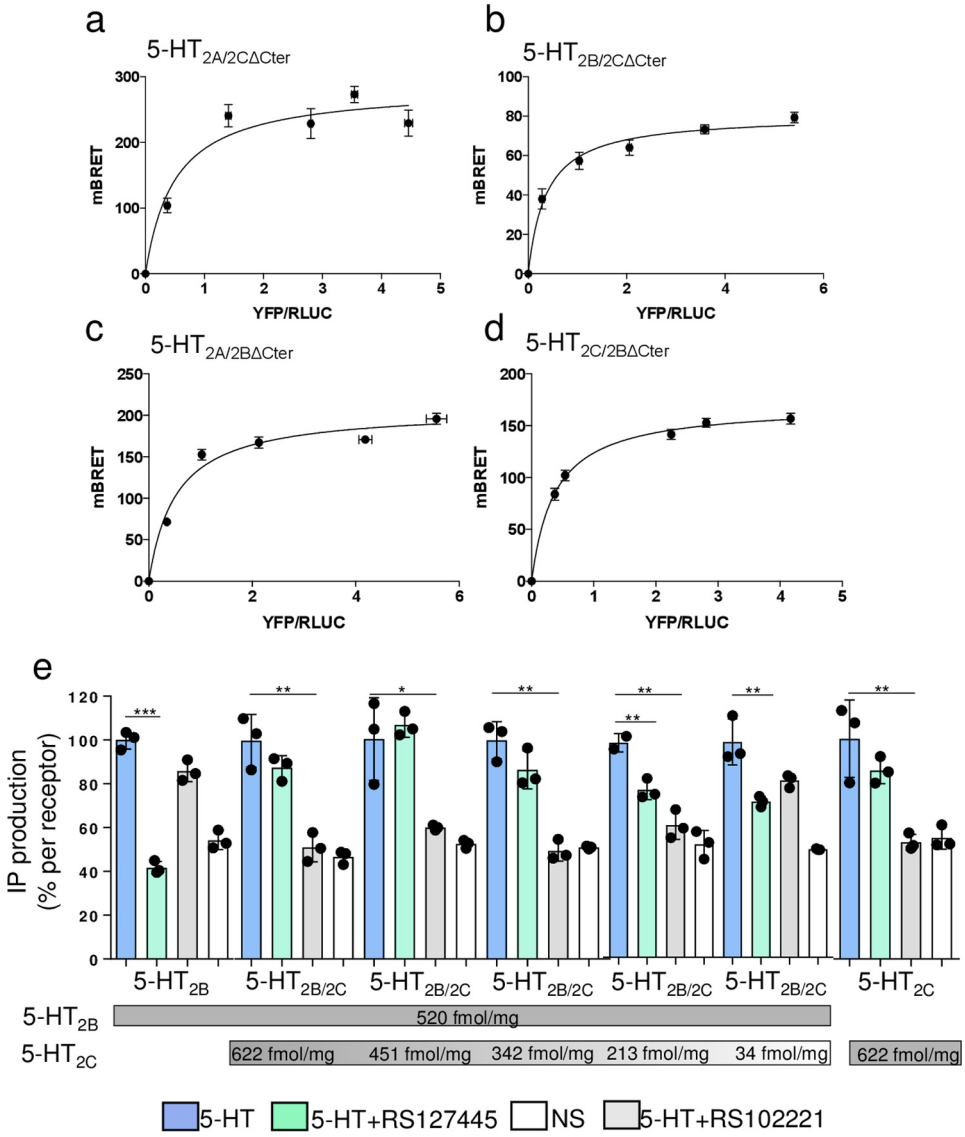

Figure 7. *a–d,* constitutive heterodimerization of 5-HT$_2$ receptors with 5-HT$_{2B\Delta Cter}$ and 5-HT$_{2C\Delta Cter}$ constructs in living HEK293 cells. HEK293 cells were co-transfected with plasmids coding for a constant amount of RLuc-5-HT$_{2A}$, RLuc-5-HT$_{2B}$, or RLuc-5-HT$_{2C}$ (BRET donors) and increasing concentrations of YFP tagged ΔCter constructs (the BRET acceptor). Energy transfer was measured after addition of membrane-permeable luciferase substrate coelenterazine-h. The BRET signal was determined by calculating the ratio of light emitted at 530 nm and that emitted at 485 nm, as described under "Experimental procedures." *Error bars* indicate S.E. of specific BRET-ratio values obtained from triplicate determinations. BRET values (B_{max}, BRET$_{50}$) were obtained from three independent experiments. Plots were established using GraphPad software. *a,* 5-HT$_{2A/2C\Delta Cter}$: BRET$_{max}$ 284 ± 27, BRET$_{50}$ 0.49 ± 0.22; *b,* 5-HT$_{2B/2C\Delta Cter}$: BRET$_{max}$ 80 ± 3, BRET$_{50}$ 0.36 ± 0.07; *c,* 5-HT$_{2A/2B\Delta Cter}$: BRET$_{max}$ 207 ± 12, BRET$_{50}$ 0.52 ± 0.13; *d,* 5-HT$_{2C/2B\Delta Cter}$: BRET$_{max}$ 170.0 ± 2.5, BRET$_{50}$ 0.37 ± 0.02. *e,* dose dependence of 5-HT$_{2C}$ blunting effect. Progressive reduction of the 5-HT$_{2C}$ receptor cDNA transfection (from 5 μg of DNA corresponding to 622 fmol/mg to 0.1 μg of DNA corresponding to 34 fmol/mg, as determined by radioligand binding assay) revealed the sensitivity of IP production to 5-HT$_{2B}$ receptor antagonism (starting from 213 fmol/mg). The 5-HT$_{2B}$ receptor expression was constant for each condition (5 μg of DNA corresponding to 520 fmol/mg). Data are expressed as % of maximal agonist response for each transfected condition. *Bars* represent ±S.D. of three independent experiments. *NS,* non-stimulated. Data were analyzed with one-way ANOVA within each independent transfection and a Bonferroni's multiple comparisons test. *, $p < 0.05$; **, $p < 0.01$; ***, $p < 0.001$: significantly different from 5-HT stimulation.

naling, consistent with the absence of 5-HT$_{2A}$ or 5-HT$_{2B}$ monomers or homodimers at the cell surface. The analysis of BRET$_{50}$ values in saturation BRET experiments, which reflect the propensity of association between protomers, suggests that in cells expressing simultaneously 5-HT$_{2C}$ and another 5-HT$_2$ receptor isoform the heterodimers are more likely to form than homodimers or monomers, and our cytometry analysis revealed that there was no impact of plasma membrane accessibility of 5-HT$_2$ receptor protomers.

Although many reports addressing the capacity of GPCRs to form heterodimeric complexes were based on investigations performed in transfected cells, only a few studies could document the existence and the functional significance of these complexes *in vivo* (21, 29, 47). Here, we show that the expression of exogenous 5-HT$_{2C\Delta Cter}$ receptors in PFC is associated with a dramatic inhibition of 5-HT$_{2A}$ receptor-dependent ligand binding, suggesting that both receptors are able to form heterodimers *in vivo*. Accordingly, we found that virus-mediated exogenous expression of the inactive protomer 5-HT$_{2C\Delta Cter}$ reduces 5-HT$_{2A}$ receptor-dependent neuronal inhibition of DR 5-HT neurons. Altogether, these results support that 5-HT$_{2C}$ receptors are able to form functional

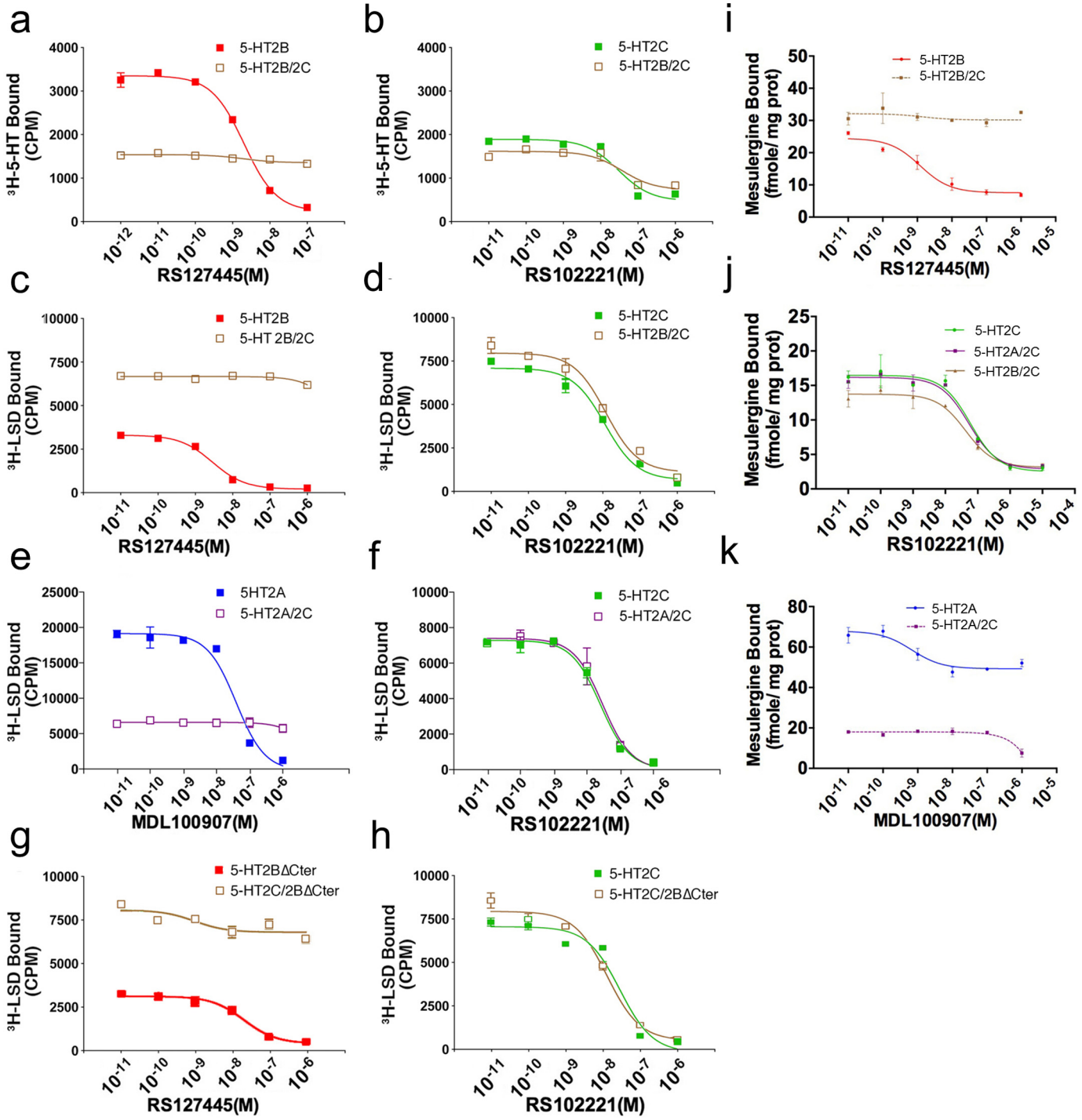

Figure 8. Co-expression of 5-HT$_{2C}$ receptors blunts 5-HT$_{2A}$ and 5-HT$_{2B}$ ligand binding. Transiently transfected cells were incubated with 5-[^{3}H]HT (*a* and *b*); [^{3}H]LSD (*c–h*); or [^{3}H]mesulergine and increasing concentrations of the 5-HT$_{2A}$ or 5-HT$_{2B}$ antagonist or 5-HT$_{2C}$ antagonist (*i–k*). *a* and *b*, 5-HT$_{2C}$ receptor transfection with 5-HT$_{2B}$ receptors abolishes the 5-[^{3}H]HT competition by 5-HT$_{2B}$ antagonist. *c–f*, 5-HT$_{2C}$ receptor transfection with 5-HT$_{2A}$ or 5-HT$_{2B}$ receptors abolishes the [^{3}H]LSD competition by 5-HT$_{2A}$ or 5-HT$_{2B}$ antagonists. *g* and *h*, 5-HT$_{2C}$ receptor transfection with 5-HT$_{2B\Delta Cter}$ receptors abolishes the [^{3}H]LSD competition by the 5-HT$_{2B}$ antagonist but not the 5-HT$_{2C}$ antagonist. *i–k*, 5-HT$_{2C}$ receptor transfection with 5-HT$_{2A}$ or 5-HT$_{2B}$ receptors abolishes the [^{3}H]mesulergine competition by 5-HT$_{2A}$ or 5-HT$_{2B}$ antagonists. These are representative curves of at least three independent experiments performed in duplicate, and *error bars* indicate S.E.

heterodimers with 5-HT$_{2A}$ or 5-HT$_{2B}$ receptors when co-expressed in neurons and pinpoint the physiological relevance of a putative switch in the pharmacological profile of these neurons, depending on 5-HT$_{2C}$ expression levels.

In line with this hypothesis, a recent study showed that high phenotypic motor impulsivity was associated with a diminished PFC 5-HT$_{2A}$·5-HT$_{2C}$ receptor complex (8). Independent findings about 5-HT$_{1A}$·5-HT$_7$ heterodimers (29) demonstrated that heterodimerization markedly decreases the ability of the 5-HT$_{1A}$ receptor to activate G-protein in hippocampal neurons. Interestingly, because 5-HT$_7$ receptor expression decreases during postnatal development, the concentration of

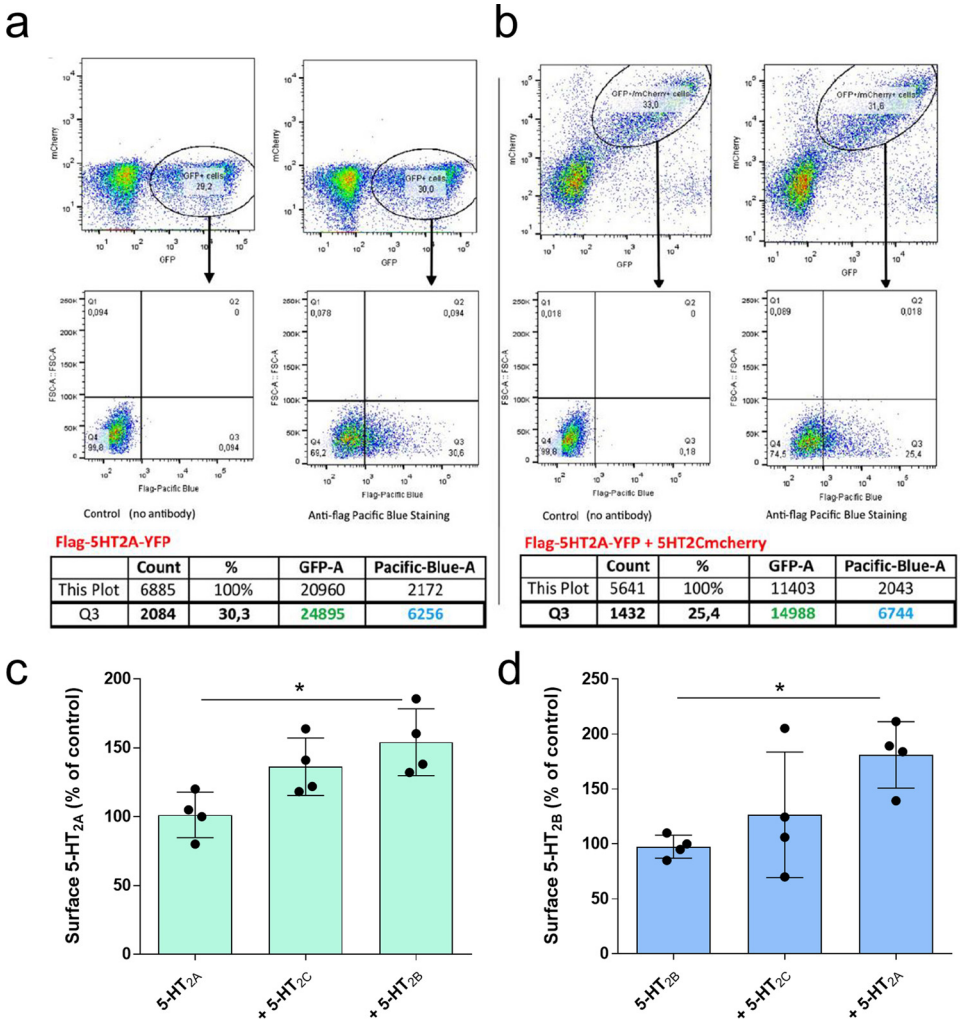

	Count	%	GFP-A	Pacific-Blue-A
This Plot	6885	100%	20960	2172
Q3	2084	30,3	24895	6256

	Count	%	GFP-A	Pacific-Blue-A
This Plot	5641	100%	11403	2043
Q3	1432	25,4	14988	6744

Figure 9. Receptor cell-surface export of 5-HT$_{2A}$ and 5-HT$_{2B}$ receptors is not affected by the co-expression with the 5-HT$_{2C}$ protomer. Surface 5-HT$_{2A}$ or 5-HT$_{2B}$ receptors in YFP-Cherry positive non-permeabilized cells were quantified by cytometry using anti-FLAG primary antibody conjugated to Pacific Blue dye. *a* and *b*, example of cell population analyzed for 5-HT$_{2A}$ receptor GFP and 5-HT$_{2C}$ receptor mCherry expression. Double-transfected cells (GFP$^+$/mCherry$^+$) were selected. FLAG-Pacific Blue staining (surface receptor expression) was analyzed on GFP$^+$/mCherry$^+$ cells. *Q3* shows % of Pacific Blue-positive cells. Ratio of cell-surface receptors over total were obtained (mean of Pacific Blue signal/mean of GFP) for each condition and normalized as percentage of 5-HT$_{2A}$ or 5-HT$_{2B}$ receptor alone (single transfection). *c*, FLAG-5-HT$_{2A}$-YFP alone or co-expressed with 5-HT$_{2B}$-Cherry or 5-HT$_{2C}$-Cherry. *d*, FLAG-5-HT$_{2B}$-YFP alone or co-expressed with 5-HT$_{2A}$-Cherry or 5-HT$_{2C}$-Cherry. Cell-surface 5-HT$_{2A}$ and 5-HT$_{2B}$ expression is shown by the histograms: *bars* indicate S.D. from three independent experiments. Data were analyzed with one-way ANOVA and a Bonferroni's multiple comparison test. *, $p < 0.05$ significantly different from control (receptor alone).

heterodimers and their functional significance should change over time. Similarly, it has been demonstrated that the expression of the 5-HT$_{2A}$ and 5-HT$_{2C}$ receptors varied during prenatal and early postnatal development (48), which represents a critical period for synaptogenesis and synaptic refinement (49). The 5-HT$_{2C}$ receptor is transiently expressed in the cortices from P10 to P28, whereas the 5-HT$_{2A}$ receptor expression increases progressively from P3 to P21, reaching the adult level. During the early postnatal period, pyramidal cells of layer V of the prefrontal cortex are profoundly depolarized by 5-HT, an effect that is mediated by the activation of the 5-HT$_{2A}$ receptor. However, 5-HT$_{2A}$ receptor-induced depolarization declines with increasing age (50, 51). In light of our results, 5-HT may progressively bind to the 5-HT$_{2C}$ protomer leading to a switch in signaling pathway activation and downstream membrane depolarization.

The operational model revealed no significant differences in the coupling ability to the Gα_q pathway between membranes expressing 5-HT$_2$ receptors alone and membranes expressing 5-HT$_2$ heterodimers. However, heterodimerization may affect the 5-HT$_2$ receptors signaling in many other ways; in addition to the activation of Gα_q, G$\alpha_{i/o}$, or G$\alpha_{12/13}$ proteins, activation of phospholipase A$_2$, and phospholipase D (ERK1/2 or β-arrestin-dependent pathways) (52, 53) can be mediated by 5-HT$_2$ receptors. All these pathways could be differentially affected by heterodimers. Interacting proteins like PSD-95, MUPP-1, and RSK2 (54) on 5-HT$_{2A}$ and 5-HT$_{2B}$ receptors might have also been affected by the dimerization with the 5-HT$_{2C}$ receptor. For example, the 5-HT$_{2C}$ and 5-HT$_{2B}$ receptors co-expressed in POMC neurons of the arcuate nucleus (11) are involved in feeding behavior but are not necessarily dependent on G$_q$ coupling. Additional studies on other signaling pathways should be performed to ascertain putative changes in 5-HT signaling associated with heterodimerization.

Another consequence of the dominant effect of the 5-HT$_{2C}$ receptor is a putative misleading link between pharmacological

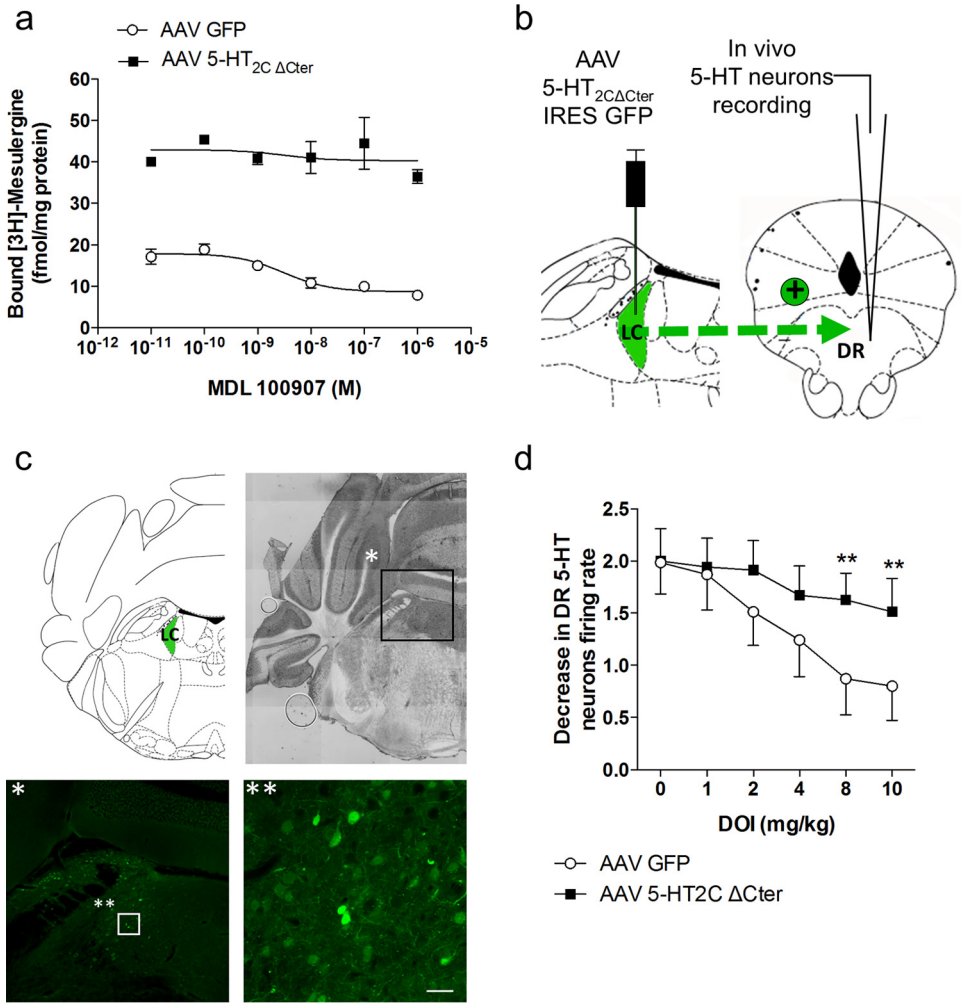

Figure 10. 5-HT$_{2C\Delta Cter}$-inactive protomer prevents 5-HT$_{2A}$ ligand binding in the PFC and reduces DOI-induced 5-HT$_{2A}$ receptor-dependent decrease of 5-HT neuron-firing rate. *a,* exogenous 5-HT$_{2C\Delta Cter}$ expression in PFC, upon bilateral infection with adeno-associated viruses carrying a 5-HT$_{2C\Delta Cter}$ construct (AAV-5-HT$_{2C\Delta Cter}$), was associated with a dramatic reduction of endogenous 5-HT$_{2A}$-dependent ligand binding compared with AAV-mediated GFP expression only. Representative example of [^{3}H]mesulergine binding (heterologous competition displacement with a selective 5-HT$_{2A}$ antagonist MDL100907) experiments performed on membrane preparation from one PFC. *Bars* represent ± S.E. from triplicates. Binding curve was done using GraphPad software. *b,* WT mice were bilaterally injected with AAV 5-HT$_{2C\Delta Cter}$ IRES GFP in the LC sending excitatory projections (*green arrow*) into the DR nucleus as shown in the diagram. After a 1-month recovery and transgene expression, *in vivo* recording of serotonin (5-HT) neurons in the DR was done. *c,* mouse brains were examined to verify the distribution of adenovirus-encoded 5-HT$_{2C\Delta Cter}$ and GFP in the LC. Fluorescence imaging of GFP in LC neurons is shown at increasing magnifications. The boxed * and ** correspond to magnified areas (*black* and *white square*). *d,* effect of the 5-HT$_{2A}$ receptor agonist DOI on the firing rate of DR 5-HT neurons in WT mice. DOI was administered using a cumulative dosing regimen, *i.e.* all mice received 1, 2, 4, 8, and 10 mg/kg (s.c.) with a 3-min interval between each injection. Data are presented as means ± S.E. of basal firing rate in mice injected with the control AAV (*open circle*) or AAV 5-HT$_{2C\Delta Cter}$ (*dark square*) ($n = 7$ mice per group). Data were analyzed with two-way ANOVA and a Bonferroni's multiple comparison test. **, $p < 0.01$: significantly different from sham AAV control-injected mice. *Scale bars,* 20 μm.

brain mapping expression and function of 5-HT$_2$ receptors. For example, in the *Globus pallidus*, the expression of 5-HT$_{2A}$ receptors, revealed by immunolabeling, had previously gone unnoticed due to absent or weak ligand binding. The 5-HT$_{2A}$ receptor immunostaining of the amygdala complex and in Purkinje cells of the cerebellum (55, 56) was also inconsistent with negative radioligand binding results previously reported (5, 57, 58). The reason for this expression discrepancy is unclear, but knowing that all these nuclei also express 5-HT$_{2C}$ receptors (4–6, 55, 59), a plausible explanation would be a pharmacological shielding of 5-HT$_{2A}$ by 5-HT$_{2C}$ receptors, without consequence for the immunocytochemistry detection. More importantly, pharmacological studies targeting 5-HT$_{2A}$ or 5-HT$_{2B}$ receptors in a physiological or a pathological context, like schizophrenia, food intake disorders, or depression, should take into account this dominant effect when brain areas of interest (*i.e.* frontal cortex, hypothalamus, or raphe nucleus, respectively) also express 5-HT$_{2C}$ receptors (8, 11, 47, 60, 61). This could lead to a misinterpretation of experimental results due to a mismatch between the consistent expression of 5-HT$_{2A}$ or 5-HT$_{2B}$ receptor in a particular nucleus, dedicated to a specific physiological function, and a lack of effect of selective pharmacological compounds. The putative formation of these heterodimers must now be taken into account when analyzing the physiological and/or pathophysiological role of 5-HT in tissues co-expressing 5-HT$_{2C}$/5-HT$_{2A}$ or 5-HT$_{2C}$/5-HT$_{2B}$ receptors.

Experimental procedures

Animals

Male mice (8–12 weeks old) used in these experiments are in a 129S2/SvPAS background (Charles River, France). Animals

were housed in groups of 3–5 per cage. The temperature was maintained at 21 ± 1 °C, under 12:12 h light/dark. Food for laboratory mice (SAFE A03, France; 3200 kcal/kg, moisture 12%, proteins 21%, lipids 5%, carbohydrates 52%, fibers 4%, and mineral ash 6%) and water were available *ad libitum*. Electrophysiological recording and animal care were conducted in accordance with the standard ethical guidelines ("Guide for the Care and Use of Laboratory Animals" from the National Institutes of Health and the European Communities Council European Communities Directive 86/609 EEC). All experiments involving mice were approved by the local ethical committee (number 1170.01).

Plasmid constructs

Human 5-HT$_{2A}$, 5-HT$_{2B}$, 5-HT$_{2CINI}$ receptor cDNAs were subcloned into the p513 vector, a derivative of the pSG5 mammalian expression vector (62), which replicates in SV40 T antigen-expressing cells and drives 5-HT receptor expression under the control of the SV40 early promoter. The C terminus truncated after amino acid 370 for the human 5-HT$_{2C}$ and amino acid 393 for the human 5-HT$_{2B}$ receptors (63) was generated by PCR deletion mutagenesis. 5-HT receptor-coding regions were amplified from their respective cDNAs using appropriate sense and antisense primers. The fragments were then subcloned in-frame in either a plasmid encoding C-terminal YFP (Clontech and BD Biosciences), N-terminal FLAG (Clontech and BD Biosciences), or Rluc. The coding regions of all constructs were entirely sequenced.

Cloning of mouse 5-HT$_{2C}$ receptor cDNA

From the full-length cDNA sequence of 5-HT$_{2CVNV}$ and 5-HT$_{VNI}$ receptors from mice that we previously reported (60), we selected the VNV-edited isoforms of 5-HT$_{2C}$ receptor for AAV injections, as VNV has been shown to be the most prevalent in C57BL/6J and 129S1/SvImJ mice (64). The C terminus of the mouse 5-HT$_{2CVNV}$ was truncated after amino acid 370.

Cell culture

COS-7, HEK293, LMTK$^-$, and CHO cells were cultured as monolayers in Dulbecco's modified Eagle's medium (DMEM) (Gibco, Invitrogen) supplemented with 10% fetal calf serum (Biowest) and 1% penicillin/streptomycin (Sigma), in 9-cm dishes (Falcon). Cells were incubated at 37 °C in a 5% CO_2 atmosphere. Cells were 80% confluent when transfected with 10 μg of DNA using nanofectin (PAA), according to the manufacturer's protocol, in an antibiotic-free medium. Four hours later, medium was replaced with fresh medium. Twenty four hours after transfection, cells were incubated in serum-free medium for membrane radioligand binding or trypsinized (trypsin 1× 0.05% EDTA, Invitrogen) and plated onto 24-well plates for IP accumulation.

AAV-mediated local LC or PFC 5-HT$_{2C\Delta Cter}$ expression

Adeno-associated virus (AAV9)-expressing GFP (7.5×10^{12} virus molecules/ml) and 5-HT$_{2C\Delta Cter}$ (IRES) GFP (8.8×10^{12} virus molecules/ml) under the control of the synapsin promoter (UNC Vector Core, Dr. R. Jude Samulski, Chapel Hill, NC) were stereotaxically injected into the LC (100 nl) or the PFC (600 nl). Mice were anesthetized with ketamine (50 mg/kg) and xylazine (2 mg/kg) and fixed in a stereotaxic apparatus. A burr hole was drilled above the LC (coordinates: 5.4 mm posterior to bregma, 1 lateral to midline) or the PFC (coordinates: 1.8 mm anterior to bregma, 2 lateral to midline). Stereotaxically guided injections were made through the hole in the dorsal surface of the cranium (3 mm deep for the LC and 1 mm for the PFC). Glass capillary tubes were pulled (HEKA pipette puller PIP5) and tips broken to 40-μm diameters. After 4 weeks of recovery and viral expression, the LC and PFC AAV-injected mice were used for electrophysiological or binding experiments, respectively. Proper viral infection was verified by GFP detection on brain-fixed sections.

In vivo electrophysiology of DR 5-HT neurons

Mice were anesthetized with chloral hydrate (400 m/kg; i.p.) and mounted in a stereotaxic frame. Additional anesthesia (50–100 mg/kg; i.p.) was given as necessary to maintain a full anesthetic state, characterized by the absence of response to a tail pinch. Body temperature was maintained at 37 °C throughout the experiments using a thermistor-controlled heating pad (Astro-Med, Elancourt, France). The extracellular recordings of the 5-HT neurons in the DR were performed using single-barreled glass micropipettes (Stoelting, Dublin, Ireland) pulled on a pipette puller (Narishige, Tokyo, Japan) preloaded with a 2 M NaCl solution. Their impedance typically ranged between 2.5 and 5 megohms. The single-barreled glass micropipettes were positioned 0.2–0.5 mm posterior to the interaural line on the midline and lowered using a hydraulic micropositioner (Kopf Instruments) into the DR, usually attained at a depth between 2.5 and 3.5 mm from the brain surface. To increase the signal-to-noise ratio, we used a current amplifier (BAK Electronics, Mount Airy, MD) connected to the active filter Humbug (Quest Scientific, DIPSI, Châtillon, France). The presumed DR 5-HT neurons were then identified according to the criteria of Aghajanian and Vandermaelen (65), *i.e.* a slow (0.5–2.5 Hz) and regular firing rate and long-duration (2–5 ms) bi- or triphasic extracellular waveform. Neuronal activity was recorded in real time using Spike2 software (Cambridge Electronic Design, Cambridge, UK), which was also used to analyze neurons off line. For all dose-response curves, only one neuron was recorded and tested from each animal.

^{3}H-radioligands and drugs

myo-[^{3}H]Inositol (51.0 Ci/mmol), [^{3}H]mesulergine (99 Ci/mmol), 5-[^{3}H]hydroxytryptamine (80.0 Ci/mmol), and [^{3}H]lysergic acid diethylamide (50.0 Ci/mmol) were purchased from PerkinElmer Life Sciences. (+)-Norfenfluramine hydrochloride (Sigma, France), RS127445 (Tocris), SB242084 (Sigma), 5-HT, DOI, mesulergine hydrochloride (Tocris), MDL100907 (Tocris), RS102221 (Tocris), and SB242084 (Tocris) were dissolved in DMSO as stock solution (1 mg/ml).

[^{3}H]IP accumulation assay

Twenty four hours before the experiment, cells were incubated in 24-well plates overnight with 20 nM *myo*-[^{3}H]inositol diluted in an inositol-free medium (BME, Lonza, Basel, Switzerland). Just before receptor stimulation, medium was

replaced by Krebs-Ringer/Hepes buffer (130 mM NaCl, 1.3 mM KCl, 2.2 mM $CaCl_2$, 1.2 mM NaH_2PO_4, 1.2 mM $MgSO_4$, 10 mM Hepes, 10 mM glucose, pH 7.4) supplemented with 20 mM LiCl to prevent IP_1 degradation. Cells were stimulated in duplicate in a final volume of 500 μl for 2 h. The experiment was stopped by replacing the stimulation medium with 10^{-3} M formic acid at room temperature for 20 min and at 4 °C overnight. Thus, IP_1 accumulated from IP_3 and IP_2 hydrolysis was released from lysed and fixed cells. The accumulated IP_1 was eluted on anion exchange columns (AG-1X8, Bio-Rad) with 0.2 M ammonium formate in 0.1 M formic acid. Scintillation mixture (Ultima Gold XR, PerkinElmer Life Sciences) was added to the eluted [^{3}H]IP sample, and radioactivity was counted in a Beckman Coulter scintillation counter. At least three independent experiments were performed in triplicate.

HTRF IP accumulation

COS-7 cells were transfected with 3 μg of DNA (1:1 ratio for co-transfection) in 6-well plates using Genjuice transfectant reagent in complete medium. Twenty four hours later the cells were trypsinized (trypsin 1× 0.05% EDTA; Invitrogen) and plated in 96-well plates (30,000 cells/well). The next day, complete medium was replaced by serum-free medium. The day of the experiment, media were replaced by stimulation buffer with LiCl to prevent IP_1 degradation (NaCl 146 mM, KCl 4.2 mM, $MgCl_2$ 0.5 mM, $CaCl_2$ 1 mM, Hepes 10 mM, glucose 5.5 mM, LiCl 50 mM, pH 7.4). Cells were stimulated during 2 h at 37 °C with a different concentration of full and partial agonists, 5-HT and DOI, respectively (10^{-11} to 10^{-6} M in stimulation buffer). Stimulation solution was replaced by lysis buffer (IP one HTRF Kit, Cisbio, France) during 1 h. Lysates were distributed to 384-well plates, and IP was labeled using HTRF reagents. The assay is based on a competitive format involving a specific antibody labeled with terbium cryptate (donor) and IP coupled to d_2 (acceptor). After a 1-h incubation with HTRF reagent, the plate was read using Mithras LB940 plate reader according to the manufacturer's instructions. At least five independent experiments were performed in duplicate.

Operational model

Data obtain in HTRF were transformed in femtomoles of IP per mg of protein per well using a standard dose-response curve. An operational model first described by Black and Leff in 1983 (31) was used to calculate coupling efficiency of each receptor in each condition for full (5-HT) and partial (DOI) agonists. This model allowed us to determine whether the dimerization could affect the coupling efficiency of the complex to the $G\alpha_q$/phospholipase C (PLC)/IP pathway. The power of a ligand to activate a specific cellular pathway is represented by the τ/K_A or RA (activity ratio). These values are extracted from the description of Model 1 and Equation 1,

$$\text{response A} = [A]^n\tau^n Em/[A]^n\tau^n + ([\text{A}] + K_A)^n$$

Model 1

where E_m is maximal response; n is slope; K_A is equilibrium constant dissociation of the agonist-receptor complex or affinity; τ is efficacy.

$$\text{RA} = \tau^n((2 + \tau^n)^{1/n} - 1)\,E_m/K_A(1 + t^n) \qquad \text{(Eq. 1)}$$

The operational model conditions show that for dose-response curves of unit slope ($n = 1$), it can be seen that RA reduces to the term E_m (τ/K_A). Ratios of these terms for particular agonists cancel the E_m term and are therefore system-independent. A theoretically complete term to describe the power of a ligand to active a cellular pathway is τ/K_A, which incorporates both elements of efficacy and affinity. Considering that the most common difference between systems is receptor density, ratios of τ/K_A account for these and are system-independent measures of the relative capacity of ligands to activate a specific pathway.

Radioligand binding assays on PFC

PFC freshly dissected from mouse brain was homogenized with 50 ml of ice-cold buffer per g of wet tissue containing 50 mM Tris and 5 mM $MgCl_2$, pH 7.4. The homogenate was centrifuged for 20 min at 15,000 × *g*. The pellet was resuspended and centrifuged under the same condition three times. Membrane preparations were resuspended in binding buffer to obtain a final concentration of 1 mg of protein/well. Radioligand binding assays were set up in a 96-well plate (1.2 ml/well capacity) using 5 nM [^{3}H]mesulergine (PerkinElmer Life Sciences) and increasing concentrations of MDL100907 for 60 min at room temperature. [^{3}H]Mesulergine ligand choice was based on the selective 5-HT$_2$ receptor-binding properties. This allows for the simultaneous measurement of 5-HT$_{2A}$ and 5-HT$_{2C}$ receptor expression, using the specific cold antagonists.

Membrane radioligand binding assay

Membrane binding assays were performed on transfected cells plated in 10-cm dishes. Cells were first washed with PBS, scraped into 10 ml of PBS on ice, and then centrifuged for 5 min at 1000 × *g*. Cell pellets were dissociated and lysed in 2 ml of binding buffer (50 mM Tris-HCl, 10 mM $MgCl_2$, 0.1 mM EDTA, pH 7.4) and centrifuged for 30 min at 10,000 × *g*. Membrane preparations were then resuspended in binding buffer to obtain a final concentration of 0.2–0.4 mg of protein/well. Aliquots of membrane suspension (200 μl/well) were incubated with 25 μl/well of ^{3}H-radioligand at a final concentration near the K_D value, diluted in binding buffer and 25 μl/well of increasing concentrations of homologous or heterologous compound (from 10^{-11} to 10^{-5} M, diluted in binding buffer) in 96-well plates for 60 min at room temperature. Membranes were harvested by rapid filtration onto Whatman GF/B glass fiber filters (Brandell) pre-soaked with cold saline solution and washed three times with cold saline solution to reduce nonspecific binding. Filters were placed in 6-ml scintillation vials and allowed to dry overnight. The next day, 4 ml of scintillation mixture were added to the samples, which were counted as before. Data in disintegrations/min were converted to femtomoles and normalized to protein content (ranging from 0.1 to 1 mg/well). At least three independent experiments were performed in duplicate.

Non-permeabilized whole cell radioligand binding assay

Cells expressing 5-HT$_{2B}$, 5-HT$_{2B\Delta Cter}$, 5-HT$_{2C}$, or 5-HT$_{2C\Delta Cter}$ receptors were plated in 24-well clusters. Twenty four hours

before the experiment, the cells were incubated in serum-free medium overnight. The next day, the medium was replaced by 400 μl/well of Krebs-Ringer/Hepes buffer (130 mM NaCl, 1.3 mM KCl, 2.2 mM $CaCl_2$, 1.2 mM NaH_2PO_4, 1.2 mM $MgSO_4$, 10 mM Hepes, 10 mM glucose, pH 7.4). Then, 50 μl of [^{3}H]mesulergine were diluted in Krebs-Ringer/Hepes buffer at a final concentration between half the K_d and the K_d for each 5-HT receptor. The radioligand was competed with 50 μl of increasing concentrations of non-radioactive ligand, also diluted in Krebs-Ringer/Hepes buffer. Cells were then incubated for 30 min at room temperature and then washed twice on ice with cold PBS. Washed cells were solubilized by the addition of 500 μl of SDS 1%. The next day, 4 ml of scintillation mixture were added to the samples, and the radioactivity was counted using a scintillation counter (Beckman Coulter). Data in disintegrations/min were converted to femtomoles and normalized to protein content (0.2–0.4 mg of protein/well). At least three independent experiments were performed in duplicate.

Co-immunoprecipitation

FLAG-tagged 5-HT$_{2B}$ and 5-HT$_{2C}$ receptor cDNA constructs were transfected in COS-7 cells with various combinations of YFP-tagged 5-HT$_2$ receptors. After 48 h, cells were washed in PBS, sonicated, and solubilized in lysis buffer (75 mM Tris, 2 mM EDTA, 12 mM $MgCl_2$, 10 mM CHAPS, protease inhibitor mixture EDTA free, pH 7.4) during 12 h at 4 °C. Lysates were centrifuged at 12,000 $\times$ *g* during 30 min at 4 °C. Immunoprecipitations were performed using EZview Red FLAG M2 affinity gel (Sigma) according to the manufacturer's recommendations. Immunoprecipitated proteins and 100 μg of total proteins were combined with Laemmli buffer, heated at 70 °C for 10 min, and run on 10% BisTris gel. Immunoblots were probed with rabbit anti-GFP (Abcam) or anti-FLAG rabbit (Sigma) antibodies diluted 1:2000, and immunoreactivity was revealed using secondary antibody coupled to 680-nm fluorophores using the Odyssey LI-COR infrared fluorescent scanner.

BRET assays

BRET assays were performed according to published methods (66). Briefly, HEK cells (5×10^5 per well of a 6-well plates) were transfected with 30–100 ng of plasmid DNA coding for the BRET donor (5-HT$_2$-Luc) and increasing amounts of BRET acceptor plasmids (5-HT$_2$-YFP; 100–4000 ng per well). Twenty four hours after transfection, cells were washed in PBS, detached using 10 mM EDTA in PBS, centrifuged (1400 $\times$ *g* for 5 min), resuspended in Hanks'-balanced salt solution, and distributed in 96-well plates (PerkinElmer Life Sciences plates; 10^5 cells per well). After addition of the luciferase substrate, coelenterazine-h (5 μM final concentration), luminescence, and fluorescence were measured simultaneously (at 485 and 530 nm, respectively) in a Mithras LB940 plate reader. The BRET ratio was calculated as ((emission at 530 nm/emission at 485 nm) − (background at 530 nm/background at 485 nm)), where background corresponds to signals in cells expressing the Rluc fusion protein alone under the same experimental conditions. For better readability, results were expressed in milli-BRET units (mBRET), with 1 mBRET corresponding to the BRET ratio multiplied by 1000. BRET ratios were plotted as a function of ((YFP − YFP0)/YFP0)/(Rluc/Rluc0), where YFP is the fluorescence signal at 530 nm after excitation at 485 nm, and Rluc is the signal at 485 nm after addition of coelenterazine-h. YFP0 and Rluc0 correspond to the same values in cells expressing the Rluc fusion protein alone.

Receptor cell-surface export analysis

To study the putative impact of 5-HT$_{2C}$ receptor co-expression on 5-HT$_{2A}$ or 5-HT$_{2B}$ receptor targeting at the cell surface, COS-7 cells were transiently co-transfected with 5-HT$_{2C}$-mCherry or 5-HT$_{2A}$-mCherry and a construct coding for 5-HT$_{2A}$ or 5-HT$_{2B}$ displaying the FLAG epitope at the N terminus and fused C-terminally to the YFP. Empty vector, p513, was used to maintain identically the total amount of transfected DNA. 48 h after transfection, cells were harvested, washed in PBS, and fixed in 4% paraformaldehyde. The expression of each receptor was assessed by measuring GFP and mCherry fluorescence using a Miltenyi MacsQuant VYB cytometer. These determinations allowed us to quantify the amount of single-transfected cells (less than 5%) of double-transfected cells (60%) and show that these values are identical whatever the combination of transfected receptors. To determine cell surface 5-HT$_{2A}$ or 5-HT$_{2B}$ expression, cell aliquots were stained with a primary antibody directed against the extracellular FLAG epitope conjugated to Pacific Blue dye (Cell Signaling) following the manufacturer's protocol. Pacific Blue and YFP signals correspond to surface and total FLAG-5-HT$_2$-YFP receptors. Cells expressing both GFP and mCherry were analyzed for Pacific Blue signal. Ratio of cell-surface receptors over total were obtained (mean of Pacific Blue signal/mean of GFP) for each condition and normalized as percentage of 5-HT$_{2A}$ or 5-HT$_{2B}$ receptor alone (single transfection), see Doly *et al.* (67).

Data analysis

Binding data were analyzed using the iterative non-linear regression model (GraphPad Prism 6.0). This allowed the calculation of inhibition constants (K_i) and the maximal number of sites (B_{max}). All values represent the average of independent experiments ± S.E. (n = number of experiments as indicated in the text).

Statistics

Comparisons between groups were performed using Student's unpaired *t* test, or one- or two-way ANOVA with Bonferroni's post hoc test were used depending on the experiment. Significance was set at $p < 0.05$ receptors.

Author contributions—S. D. and L. M. participated in research design. S. D., B. G., E. Q., and I. M. conducted the experiments. S. D., B. G., E. Q., and I. M. performed data analysis. S. D. and L. M. wrote or contributed to the writing of the manuscript.

Acknowledgment—We thank Dr. Stefano Marullo for helpful discussions and advice on BRET experiments.

References

1. Ferré, S., Baler, R., Bouvier, M., Caron, M. G., Devi, L. A., Durroux, T., Fuxe, K., George, S. R., Javitch, J. A., Lohse, M. J., Mackie, K., Milligan, G.,

Pfleger, K. D., Pin, J. P., Volkow, N. D., *et al.* (2009) Building a new conceptual framework for receptor heteromers. *Nat. Chem. Biol.* **5,** 131–134
2. Bulenger, S., Marullo, S., and Bouvier, M. (2005) Emerging role of homo- and heterodimerization in G-protein-coupled receptor biosynthesis and maturation. *Trends Pharmacol. Sci.* **26,** 131–137
3. Millan, M. J., Marin, P., Bockaert, J., and Mannoury la Cour, C. (2008) Signaling at G-protein-coupled serotonin receptors: recent advances and future research directions. *Trends Pharmacol. Sci.* **29,** 454–464
4. Bonhaus, D. W., Bach, C., DeSouza, A., Salazar, F. H., Matsuoka, B. D., Zuppan, P., Chan, H. W., and Eglen, R. M. (1995) The pharmacology and distribution of human 5-hydroxytryptamine 2B (5-HT2B) receptor gene products: comparison with 5-HT2A and 5-HT2C receptors. *Br. J. Pharmacol.* **115,** 622–628
5. Pompeiano, M., Palacios, J. M., and Mengod, G. (1994) Distribution of the serotonin 5-HT2 receptor family mRNAs: comparison between 5-HT2A and 5-HT2C receptors. *Brain Res. Mol. Brain Res.* **23,** 163–178
6. Carr, D. B., Cooper, D. C., Ulrich, S. L., Spruston, N., and Surmeier, D. J. (2002) Serotonin receptor activation inhibits sodium current and dendritic excitability in prefrontal cortex via a protein kinase C-dependent mechanism. *J. Neurosci.* **22,** 6846–6855
7. Nocjar, C., Alex, K. D., Sonneborn, A., Abbas, A. I., Roth, B. L., and Pehek, E. A. (2015) Serotonin-2C and -2a receptor co-expression on cells in the rat medial prefrontal cortex. *Neuroscience* **297,** 22–37
8. Anastasio, N. C., Stutz, S. J., Fink, L. H., Swinford-Jackson, S. E., Sears, R. M., DiLeone, R. J., Rice, K. C., Moeller, F. G., and Cunningham, K. A. (2015) Serotonin (5-HT) 5-HT2A receptor (5-HT2AR):5-HT2CR imbalance in medial prefrontal cortex associates with motor impulsivity. *ACS Chem. Neurosci.* **6,** 1248–1258
9. Bubar, M. J., Stutz, S. J., and Cunningham, K. A. (2011) 5-HT(2C) receptors localize to dopamine and GABA neurons in the rat mesoaccumbens pathway. *PLoS ONE* **6,** e20508
10. Esposito, E. (2006) Serotonin-dopamine interaction as a focus of novel antidepressant drugs. *Curr. Drug Targets* **7,** 177–185
11. Yadav, V. K., Oury, F., Suda, N., Liu, Z. W., Gao, X. B., Confavreux, C., Klemenhagen, K. C., Tanaka, K. F., Gingrich, J. A., Guo, X. E., Tecott, L. H., Mann, J. J., Hen, R., Horvath, T. L., and Karsenty, G. (2009) A serotonin-dependent mechanism explains the leptin regulation of bone mass, appetite, and energy expenditure. *Cell* **138,** 976–989
12. Raymond, J. R., Mukhin, Y. V., Gelasco, A., Turner, J., Collinsworth, G., Gettys, T. W., Grewal, J. S., and Garnovskaya, M. N. (2001) Multiplicity of mechanisms of serotonin receptor signal transduction. *Pharmacol. Ther.* **92,** 179–212
13. Brea, J., Castro, M., Giraldo, J., López-Giménez, J. F., Padín, J. F., Quintián, F., Cadavid, M. I., Vilaró, M. T., Mengod, G., Berg, K. A., Clarke, W. P., Vilardaga, J. P., Milligan, G., and Loza, M. I. (2009) Evidence for distinct antagonist-revealed functional states of 5-hydroxytryptamine(2A) receptor homodimers. *Mol. Pharmacol.* **75,** 1380–1391
14. Herrick-Davis, K., Grinde, E., Harrigan, T. J., and Mazurkiewicz, J. E. (2005) Inhibition of serotonin 5-hydroxytryptamine2c receptor function through heterodimerization: receptor dimers bind two molecules of ligand and one G-protein. *J. Biol. Chem.* **280,** 40144–40151
15. Herrick-Davis, K., Grinde, E., Lindsley, T., Teitler, M., Mancia, F., Cowan, A., and Mazurkiewicz, J. E. (2015) Native serotonin 5-HT2C receptors are expressed as homodimers on the apical surface of choroid plexus epithelial cells. *Mol. Pharmacol.* **87,** 660–673
16. Herrick-Davis, K., Grinde, E., Lindsley, T., Cowan, A., and Mazurkiewicz, J. E. (2012) Oligomer size of the serotonin 5-hydroxytryptamine 2C (5-HT2C) receptor revealed by fluorescence correlation spectroscopy with photon counting histogram analysis: evidence for homodimers without monomers or tetramers. *J. Biol. Chem.* **287,** 23604–23614
17. Berthouze, M., Ayoub, M., Russo, O., Rivail, L., Sicsic, S., Fischmeister, R., Berque-Bestel, I., Jockers, R., and Lezoualc'h, F. (2005) Constitutive dimerization of human serotonin 5-HT4 receptors in living cells. *FEBS Lett.* **579,** 2973–2980
18. Xie, Z., Lee, S. P., O'Dowd, B. F., and George, S. R. (1999) Serotonin 5-HT1B and 5-HT1D receptors form homodimers when expressed alone and heterodimers when co-expressed. *FEBS Lett.* **456,** 63–67
19. Smith, C., Toohey, N., Knight, J. A., Klein, M. T., and Teitler, M. (2011) Risperidone-induced inactivation and clozapine-induced reactivation of rat cortical astrocyte 5-hydroxytryptamine(7) receptors: evidence for *in situ* G protein-coupled receptor homodimer protomer cross-talk. *Mol. Pharmacol.* **79,** 318–325
20. Pellissier, L. P., Barthet, G., Gaven, F., Cassier, E., Trinquet, E., Pin, J. P., Marin, P., Dumuis, A., Bockaert, J., Banères, J. L., and Claeysen, S. (2011) G protein activation by serotonin type 4 receptor dimers: evidence that turning on two protomers is more efficient. *J. Biol. Chem.* **286,** 9985–9997
21. Albizu, L., Holloway, T., González-Maeso, J., and Sealfon, S. C. (2011) Functional crosstalk and heteromerization of serotonin 5-HT2A and dopamine D2 receptors. *Neuropharmacology* **61,** 770–777
22. Moreno, J. L., Muguruza, C., Umali, A., Mortillo, S., Holloway, T., Pilar-Cuéllar, F., Mocci, G., Seto, J., Callado, L. F., Neve, R. L., Milligan, G., Sealfon, S. C., López-Giménez, J. F., Meana, J. J., Benson, D. L., and González-Maeso, J. (2012) Identification of three residues essential for 5-hydroxytryptamine 2A-metabotropic glutamate 2 (5-HT2A.mGlu2) receptor heteromerization and its psychoactive behavioral function. *J. Biol. Chem.* **287,** 44301–44319
23. Viñals, X., Moreno, E., Lanfumey, L., Cordomí, A., Pastor, A., de La Torre, R., Gasperini, P., Navarro, G., Howell, L. A., Pardo, L., Lluís, C., Canela, E. I., McCormick, P. J., Maldonado, R., and Robledo, P. (2015) Cognitive impairment induced by Δ9-tetrahydrocannabinol occurs through heteromers between cannabinoid CB1 and serotonin 5-HT2A receptors. *PLoS Biol.* **13,** e1002194
24. Schellekens, H., van Oeffelen, W. E., Dinan, T. G., and Cryan, J. F. (2013) Promiscuous dimerization of the growth hormone secretagogue receptor (GHS-R1a) attenuates ghrelin-mediated signaling. *J. Biol. Chem.* **288,** 181–191
25. Kamal, M., Gbahou, F., Guillaume, J. L., Daulat, A. M., Benleulmi-Chaachoua, A., Luka, M., Chen, P., Kalbasi Anaraki, D., Baroncini, M., Mannoury la Cour, C., Millan, M. J., Prevot, V., Delagrange, P., and Jockers, R. (2015) Convergence of melatonin and serotonin (5-HT) signaling at MT2/5-HT2C receptor heteromers. *J. Biol. Chem.* **290,** 11537–11546
26. Cussac, D., Rauly-Lestienne, I., Heusler, P., Finana, F., Cathala, C., Bernois, S., and De Vries, L. (2012) μ-Opioid and 5-HT1A receptors heterodimerize and show signalling crosstalk via G protein and MAP-kinase pathways. *Cell. Signal.* **24,** 1648–1657
27. Łukasiewicz, S., Błasiak, E., Faron-Górecka, A., Polit, A., Tworzydło, M., Górecki, A., Wasylewski, Z., and Dziedzicka-Wasylewska, M. (2007) Fluorescence studies of homooligomerization of adenosine A2A and serotonin 5-HT1A receptors reveal the specificity of receptor interactions in the plasma membrane. *Pharmacol. Rep.* **59,** 379–392
28. Jaffré, F., Bonnin, P., Callebert, J., Debbabi, H., Setola, V., Doly, S., Monassier, L., Mettauer, B., Blaxall, B. C., Launay, J. M., and Maroteaux, L. (2009) Serotonin and angiotensin receptors in cardiac fibroblasts coregulate adrenergic-dependent cardiac hypertrophy. *Circ. Res.* **104,** 113–123
29. Renner, U., Zeug, A., Woehler, A., Niebert, M., Dityatev, A., Dityateva, G., Gorinski, N., Guseva, D., Abdel-Galil, D., Fröhlich, M., Döring, F., Wischmeyer, E., Richter, D. W., Neher, E., and Ponimaskin, E. G. (2012) Heterodimerization of serotonin receptors 5-HT1A and 5-HT7 differentially regulates receptor signalling and trafficking. *J. Cell Sci.* **125,** 2486–2499
30. Janoshazi, A., Deraet, M., Callebert, J., Setola, V., Guenther, S., Saubamea, B., Manivet, P., Launay, J. M., and Maroteaux, L. (2007) Modified receptor internalization upon coexpression of 5-HT1B receptor and 5-HT2B receptors. *Mol. Pharmacol.* **71,** 1463–1474
31. Black, J. W., and Leff, P. (1983) Operational models of pharmacological agonism. *Proc. R. Soc. Lond. B Biol. Sci.* **220,** 141–162
32. Kenakin, T., Watson, C., Muniz-Medina, V., Christopoulos, A., and Novick, S. (2012) A simple method for quantifying functional selectivity and agonist bias. *ACS Chem. Neurosci.* **3,** 193–203
33. Doly, S., Madeira, A., Fischer, J., Brisorgueil, M. J., Daval, G., Bernard, R., Vergé, D., and Conrath, M. (2004) The 5-HT2A receptor is widely distributed in the rat spinal cord and mainly localized at the plasma membrane of postsynaptic neurons. *J. Comp. Neurol.* **472,** 496–511
34. Cornea-Hébert, V., Riad, M., Wu, C., Singh, S. K., and Descarries, L. (1999) Cellular and subcellular distribution of the serotonin 5-HT2A receptor in the central nervous system of adult rat. *J. Comp. Neurol.* **409,** 187–209

35. Boothman, L. J., and Sharp, T. (2005) A role for midbrain raphe γ-aminobutyric acid neurons in 5-hydroxytryptamine feedback control. *Neuroreport* **16,** 891–896
36. Bortolozzi, A., and Artigas, F. (2003) Control of 5-hydroxytryptamine release in the dorsal raphe nucleus by the noradrenergic system in rat brain. Role of α-adrenoceptors. *Neuropsychopharmacology* **28,** 421–434
37. Quesseveur, G., Reperant, C., David, D. J., Gardier, A. M., Sanchez, C., and Guiard, B. P. (2013) 5-HT(2)A receptor inactivation potentiates the acute antidepressant-like activity of escitalopram: involvement of the noradrenergic system. *Exp. Br. Res.* **226,** 285–295
38. Szabo, S. T., and Blier, P. (2001) Functional and pharmacological characterization of the modulatory role of serotonin on the firing activity of locus coeruleus norepinephrine neurons. *Brain Res.* **922,** 9–20
39. Szabo, S. T., and Blier, P. (2002) Effects of serotonin (5-hydroxytryptamine, 5-HT) reuptake inhibition plus 5-HT(2A) receptor antagonism on the firing activity of norepinephrine neurons. *J. Pharmacol. Exp. Ther.* **302,** 983–991
40. Maurice, P., Kamal, M., and Jockers, R. (2011) Asymmetry of GPCR oligomers supports their functional relevance. *Trends Pharmacol. Sci.* **32,** 514–520
41. Siddiquee, K., Hampton, J., McAnally, D., May, L., and Smith, L. (2013) The apelin receptor inhibits the angiotensin II type 1 receptor via allosteric trans-inhibition. *Br. J. Pharmacol.* **168,** 1104–1117
42. AbdAlla, S., Lother, H., Abdel-tawab, A. M., and Quitterer, U. (2001) The angiotensin II AT2 receptor is an AT1 receptor antagonist. *J. Biol. Chem.* **276,** 39721–39726
43. Jastrzebska, B. (2013) GPCR: G protein complexes–the fundamental signaling assembly. *Amino Acids* **45,** 1303–1314
44. Levoye, A., Dam, J., Ayoub, M. A., Guillaume, J. L., Couturier, C., Delagrange, P., and Jockers, R. (2006) The orphan GPR50 receptor specifically inhibits MT1 melatonin receptor function through heterodimerization. *EMBO J.* **25,** 3012–3023
45. Herrick-Davis, K. (2013) Functional significance of serotonin receptor dimerization. *Exp. Br. Res.* **230,** 375–386
46. Mancia, F., Assur, Z., Herman, A. G., Siegel, R., and Hendrickson, W. A. (2008) Ligand sensitivity in dimeric associations of the serotonin 5HT2c receptor. *EMBO Rep.* **9,** 363–369
47. Fribourg, M., Moreno, J. L., Holloway, T., Provasi, D., Baki, L., Mahajan, R., Park, G., Adney, S. K., Hatcher, C., Eltit, J. M., Ruta, J. D., Albizu, L., Li, Z., Umali, A., Shim, J., *et al.* (2011) Decoding the signaling of a GPCR heteromeric complex reveals a unifying mechanism of action of antipsychotic drugs. *Cell* **147,** 1011–1023
48. Li, Q. H., Nakadate, K., Tanaka-Nakadate, S., Nakatsuka, D., Cui, Y., and Watanabe, Y. (2004) Unique expression patterns of 5-HT2A and 5-HT2C receptors in the rat brain during postnatal development: Western blot and immunohistochemical analyses. *J. Comp. Neurol.* **469,** 128–140
49. Gaspar, P., Cases, O., and Maroteaux, L. (2003) The developmental role of serotonin: news from mouse molecular genetics. *Nat. Rev. Neurosci.* **4,** 1002–1012
50. Béïque, J. C., Campbell, B., Perring, P., Hamblin, M. W., Walker, P., Mladenovic, L., and Andrade, R. (2004) Serotonergic regulation of membrane potential in developing rat prefrontal cortex: coordinated expression of 5-hydroxytryptamine (5-HT)1A, 5-HT2A, and 5-HT7 receptors. *J. Neurosci.* **24,** 4807–4817
51. Béïque, J. C., Chapin-Penick, E. M., Mladenovic, L., and Andrade, R. (2004) Serotonergic facilitation of synaptic activity in the developing rat prefrontal cortex. *J. Physiol.* **556,** 739–754
52. Wacker, D., Wang, C., Katritch, V., Han, G. W., Huang, X. P., Vardy, E., McCorvy, J. D., Jiang, Y., Chu, M., Siu, F. Y., Liu, W., Xu, H. E., Cherezov, V., Roth, B. L., and Stevens, R. C. (2013) Structural features for functional selectivity at serotonin receptors. *Science* **340,** 615–619
53. Bohn, L. M., and Schmid, C. L. (2010) Serotonin receptor signaling and regulation via β-arrestins. *Crit. Rev. Biochem. Mol. Biol.* **45,** 555–566
54. Roth, B. L. (2011) Irving Page Lecture: 5-HT(2A) serotonin receptor biology: interacting proteins, kinases and paradoxical regulation. *Neuropharmacology* **61,** 348–354
55. Bombardi, C. (2014) Neuronal localization of the 5-HT2 receptor family in the amygdaloid complex. *Front. Pharmacol.* **5,** 68
56. Maeshima, T., Shutoh, F., Hamada, S., Senzaki, K., Hamaguchi-Hamada, K., Ito, R., and Okado, N. (1998) Serotonin2A receptor-like immunoreactivity in rat cerebellar Purkinje cells. *Neurosci. Lett.* **252,** 72–74
57. Pazos, A., Cortés, R., and Palacios, J. M. (1985) Quantitative autoradiographic mapping of serotonin receptors in the rat brain. II. Serotonin-2 receptors. *Brain Res.* **346,** 231–249
58. Wright, D. E., Seroogy, K. B., Lundgren, K. H., Davis, B. M., and Jennes, L. (1995) Comparative localization of serotonin1A, 1C, and 2 receptor subtype mRNAs in rat brain. *J. Comp. Neurol.* **351,** 357–373
59. Ward, R. P., and Dorsa, D. M. (1996) Colocalization of serotonin receptor subtypes 5-HT2A, 5-HT2C, and 5-HT6 with neuropeptides in rat striatum. *J. Comp. Neurol.* **370,** 405–414
60. Banas, S. M., Doly, S., Boutourlinsky, K., Diaz, S. L., Belmer, A., Callebert, J., Collet, C., Launay, J. M., and Maroteaux, L. (2011) Deconstructing antiobesity compound action: requirement of serotonin 5-HT2B receptors for dexfenfluramine anorectic effects. *Neuropsychopharmacology* **36,** 423–433
61. Diaz, S. L., Doly, S., Narboux-Nême, N., Fernández, S., Mazot, P., Banas, S. M., Boutourlinsky, K., Moutkine, I., Belmer, A., Roumier, A., and Maroteaux, L. (2012) 5-HT(2B) receptors are required for serotonin-selective antidepressant actions. *Mol. Psychiatry* **17,** 154–163
62. Green, S., Issemann, I., and Sheer, E. (1988) A versatile *in vivo* and *in vitro* eukaryotic expression vector for protein engineering. *Nucleic Acids Res.* **16,** 396
63. Deraet, M., Manivet, P., Janoshazi, A., Callebert, J., Guenther, S., Drouet, L., Launay, J. M., and Maroteaux, L. (2005) The natural mutation encoding a C-terminal truncated 5-hydroxytryptamine 2B receptor is a gain of proliferative functions. *Mol. Pharmacol.* **67,** 983–991
64. Du, Y., Davisson, M. T., Kafadar, K., and Gardiner, K. (2006) A-to-I pre-mRNA editing of the serotonin 2C receptor: comparisons among inbred mouse strains. *Gene* **382,** 39–46
65. Aghajanian, G. K., and Vandermaelen, C. P. (1982) Intracellular recording *in vivo* from serotonergic neurons in the rat dorsal raphe nucleus: methodological considerations. *J. Histochem. Cytochem.* **30,** 813–814
66. Achour, L., Kamal, M., Jockers, R., and Marullo, S. (2011) Using quantitative BRET to assess G protein-coupled receptor homo- and heterodimerization. *Methods Mol. Biol.* **756,** 183–200
67. Doly, S., Shirvani, H., Gäta, G., Meye, F. J., Emerit, M. B., Enslen, H., Achour, L., Pardo-Lopez, L., Yang, S. K., Armand, V., Gardette, R., Giros, B., Gassmann, M., Bettler, B., Mameli, M., Darmon, M., and Marullo, S. (2016) GABA receptor cell-surface export is controlled by an endoplasmic reticulum gatekeeper. *Mol. Psychiatry* **21,** 480–490